https://doi.org/10.5194/egusphere-2026-5001
Preprint. Discussion started: 11 September 2026


# Cloud condensation nuclei at two Finnish sub-Arctic sites: long-term observations of aerosol activation, predictions based on a simple semi-empirical parameterization, and comparison to global climate model simulations

Charlotte G. Stapleton[1,2], Mikko Sipilä[1], Arundathi Chandrasekharan[3], Joonas Merikanto[3], Kimmo Neitola[1,*], Tuomo Nieminen[2,4], Risto Makkonen[3], Jorma Joutsensaari[5], Aki Virkkula[3], Antti-Pekka Hyvärinen[3**]

[1] Wolfson Atmospheric Chemistry Laboratories, Department of Chemistry, University of York, York, UK

[2] Institute for Atmospheric and Earth System Research (INAR), University of Helsinki, Helsinki, Finland

[3] Finnish Meteorological Institute, Helsinki, Finland

[4] Department of Physics, University of Helsinki, Helsinki, Finland

[5] Department of Technical Physics, University of Eastern Finland, Kuopio, Finland

[*] Currently at Vaisala Oyj, Helsinki, Finland

[**] Corresponding author: antti.hyvarinen@fmi.fi

## ABSTRACT

In this study, we present long-term observations of cloud condensation nuclei (CCN) at two locations in the Finnish sub-Arctic: Pallastunturi and Värriö. Both stations belong to the ACTRIS research infrastructure. At Pallastunturi, the interactions between aerosols and clouds have been measured in situ at a fjell top, 565 m a.s.l. since 2005. From Pallastunturi data, a simple parameterisation was developed to predict the activation diameter $D_{50}$ and subsequent CCN- concentrations, based on air mass origin and temperature. The parameterization was applied to aerosol size distribution measurements conducted at Värriö from 1998 to 2021. The average annual CCN concentrations were 140 ± 40 # /cm$^3$ at Pallas and 170 ± 50 # /cm$^3$ at Värriö. The CCN- concentrations exhibited statistically significant decreasing trends at both stations: for Pallas -2.5 CCN /cm$^3$ / year, and for Värriö -4.2 CCN /cm$^3$ / year. The decrease was most pronounced during February and March, i.e. during the Arctic Haze period. We also compared the results with EC-Earth3 global climate model simulations. Using two measurement sites separated by ~230 km reduces the uncertainty in the spatial representativeness of observations and provides a robust basis for climate model evaluation. EC-Earth3 predicted the measured CCN- concentrations fairly well at 0.2% supersaturation, reproducing the observed long-term trend. However, the modelled seasonal variation was slightly different, predicting higher concentrations during winter time (November to April). The study

https://doi.org/10.5194/egusphere-2026-5001
Preprint. Discussion started: 11 September 2026


demonstrates the value of long term in-cloud aerosol measurements in validating and improving climate predictions.

## 1 INTRODUCTION

The interactions between atmospheric aerosols and clouds serve as the largest uncertainty in estimating the Earth's radiative forcing (IPCC, 2021), and hence, in predictions for climate change (Forster et al., 2007). A critical process affecting aerosol-cloud interactions is the ability of aerosol particles to act as cloud condensation nuclei (CCN), and the way these CCNs affect cloud properties. For example, high CCN- concentrations lead to smaller cloud droplets and higher albedo (Twomey, 1977); and increase cloud lifetime by suppressing precipitation (Albrecht, 1989). The ability of an aerosol particle to act as a CCN depends heavily on its size, and to a secondary degree, its chemistry (e.g. Dusek et al., 2006). Moreover, meteorology, through updraft velocity and the availability of water vapour, affect the maximum supersaturation and thus the activation efficiency of the aerosol population. This leads to aerosol-cloud interactions that are 'regime'-dependent, meaning that they can vary under different meteorological conditions (Chang et al., 2015). Based on updraft velocities and particle concentrations, Reutter et al. (2009) segregated cloud droplet formation into three regimes: an aerosol-limited regime, an updraft- limited regime, and a transitional regime. This affects for example the susceptibility of cloud droplet number concentration ($N_d$) to CCN concentration (Virtanen et al. 2025). A high susceptibility of $N_d$ to CCN is expected in the aerosol limited regime, while a low susceptibility can be expected in the updraft limited regime. As the cloud droplet formation regimes can be highly localized, high-quality observations are critical in understanding spatial differences of cloud formation, and providing observational constraints for global climate models (Wang et al., 2026).

The Arctic is one of the regions where clouds play a vital role in modulating the climate, and there is a need for more long-term comprehensive observations of aerosols and clouds (such as described in Platt et al. 2022, Koike et al., 2019 and Motos et al., 2023) in the region. As the Arctic is warming rapidly (Rantanen et al. 2022), clouds in the region can also be expected to undergo changes, highlighting the value of long-term observations.

Direct measurements of CCN- concentrations typically involve CCN- counters, which utilize pre-defined supersaturation levels for the aerosol activation to occur (Roberts and Nenes 2005). Such measurements have been conducted in several places around the world (e.g. Schmale et al., 2017), and provide gold-standard data for development and validation of climate models. The caveat of these measurements is that the predefined supersaturations do not represent real cloud base conditions

https://doi.org/10.5194/egusphere-2026-5001
Preprint. Discussion started: 11 September 2026


(where activation takes place) where supersaturation is not constant and may fluctuate substantially (Yang et al., 2019). Therefore, CCN- measurements should preferably be complemented by measurements of updraft velocity (or by other means to estimate the true supersaturation), to be able to estimate the number of cloud droplets formed.

An alternative way to include the effect of supersaturation for aerosol-cloud interaction studies, is to make the measurements directly inside a cloud. Apart from aircraft measurements, this can be conducted at ground stations (mostly mountain locations or towers) that experience clouds *in situ*. Here, sampling of aerosol particles is performed through a cloud residual inlet (Karlsson et al., 2021), or with inlets sampling the total (including cloud droplets) and interstitial (excluding cloud droplets) aerosol (Kivekäs et al., 2009). This enables quantification of the aerosol particles that acted as a real CCN, implicitly taking the cloud supersaturation effect into account. Only a few such ground stations exist worldwide (see e.g. Laj et al. 2024).

As direct CCN- measurements are scarce, parameterisation approaches based on observations have been developed to predict CCN concentrations. The parameterizations range from using simple regression proxies of CCN such as satellite-derived aerosol optical depth, AOD (e.g. Ahn et al. 2021), to employing theory-based activation schemes for measured aerosol properties; in particular the Köhler theory (Köhler, 1936) and its derivatives (e.g. Petters and Kreidenweis, 2007). Recently, Fang et al. (2016) compared seven methods for CCN parameterization based on measured total particle concentration, particle number size distribution and cloud condensation nuclei concentrations on Mt. Huang, China. They concluded that a parameterization using an average critical diameter above which particles are assumed to activate to cloud droplets, provides the best estimate of CCN. Similarly, Deng et al. (2013) recommended predicting CCN concentrations by using particle number size distributions with determined critical diameters or size-resolved activation ratios.

The impact of aerosols and their interactions with clouds are one of the main sources of uncertainty in climate models (Boucher et al. 2013). The causes of uncertainties include incorrect modelling of aerosol precursor emissions, nucleation events, as well as incorrect representation of aerosol size distributions in models (Pierce et al. 2009; Lee et al. 2013). Among the uncertainties noted in Lee et al. (2013), high latitudes during wintertime are noted as a region of high uncertainty. This long-term CCN dataset provides an opportunity to evaluate the modelled CCN along with the size distribution data.

The overarching aim of this study was to investigate the long-term CCN- concentrations in the Finnish sub-arctic, based on directly measured data from two ground-based stations. At the first station, which is regularly inside low-level clouds, aerosol activation into cloud droplets has been measured

https://doi.org/10.5194/egusphere-2026-5001
Preprint. Discussion started: 11 September 2026


routinely; while the second station is equipped with aerosol size distribution measurements that can be used as a proxy for CCN. In this study, we demonstrate how the data can be combined to predict CCN concentrations at both stations.

To be explicit, the main goals of this study were to: 1) develop a simple cloud activation parameterisation based on long-term measurements at the Pallastunturi research station (from hereafter: Pallas), enabling the derivation of the aerosol activation diameter based on prevailing atmospheric conditions, 2) apply the parameterization to predict CCN concentrations at the Värriö research station, 3) present the long-term CCN concentrations from both stations and 4) compare them against global climate model results. To the best of our knowledge, this study presents the longest (> 10 year) time series of CCN concentrations in the Arctic region.

## 2 MATERIALS AND METHODS

### 2.1 MEASUREMENT SITES

Measurements relevant to this study were conducted at Pallas Atmosphere-Ecosystem Supersite (Hatakka et al., 2003, Lohila et al. 2015), and Värriö SMEAR I (Station for Measuring Ecosystem-Atmosphere Relations) sub-arctic research station (Hari et al., 1994). Both stations belong to the European 'Aerosols, Clouds and Trace Gases Research Infrastructure', ACTRIS (Laj et al., 2024). The stations are located in Finnish Lapland (Figure 1), and their surrounding environments are very similar, being that of boreal forest with no significant local air pollution sources. The closest major sources of pollution are the smelters Montshegorsk and Nikel in the Kola Peninsula region, North-West Russia, located 140 km East and 200 km North of Värriö station (67° 45' N, 29° 36' E), respectively.

Pallas station (67° 58' N, 24° 07' E) consists of several measurement stations, of which data from the main station, Sammaltunturi, is used in this work. The station resides on the top of a hill (565 m a.s.l., about 100-250 m higher than the surrounding landscape), and is regularly inside low-level clouds, making it suitable for studies on aerosol-cloud interactions (Doulgeris et al. 2023). The distance between Pallas and Värriö is about 230 km. As there are no major local emission sources in the region, we assume that aerosol properties measured at both stations are similar and governed by long-range-transported air masses.

https://doi.org/10.5194/egusphere-2026-5001
Preprint. Discussion started: 11 September 2026



Figure 1: Map of the study area, highlighting specifically the relative locations of Pallas and Värriö research station

## 2.2 INSTRUMENTATION

At Pallas, two differential mobility particle sizers (DMPS) measured the aerosol number size distribution in the size range 7 – 500 nm, divided into 30 logarithmically spaced size bins. A complete size distribution was recorded approximately every 5.5 minutes. One DMPS system, referred to as the total DMPS, measures the concentration of all aerosol particles including the cloud droplet nuclei by evaporating the condensed water vapour, as well as the non-activated particles. The second, interstitial DMPS measures only the interstitial (non-activated) aerosol particles using an inlet cut-off (c.a. 7 µm), preventing larger, cloud activated particles from entering the instrument (Komppula et al., 2005). When the station is inside a cloud, the difference between the two recorded particle size distributions provides the size distribution of particles activated into cloud droplets, yielding the CCN-concentration, $N_{CCN}$. At the prevailing updraft velocity and supersaturation of water vapour, this can be estimated to be equal to the cloud droplet number concentration $N_d$, i.e. $N_{CCN} = N_d$. For this study, the period of 2005 – 2020 of quality assured data from both instruments simultaneously was used. On

https://doi.org/10.5194/egusphere-2026-5001
Preprint. Discussion started: 11 September 2026


occasions where there are no clouds present at the station, the size distributions recorded by the total and interstitial DMPS instruments were within instrumental uncertainties.

Various meteorological parameters, out of which specifically relevant to this study is air temperature, were recorded at Pallas by the Vaisala Milos 500 automatic weather station. Visibility was recorded by the Vaisala FD12P weather sensor. The above data were recorded as one minute means.

At Värriö, the aerosol size distribution was recorded by a DMPS instrument approximately every 10 minutes (Aalto et al., 2001) during 1998-2021. Only out-of-cloud measurements were conducted at Värriö, thus the aerosol data recorded is comparable to the total air size distribution measurements made at Pallas. The lower and upper limits of the size bins varied over the time period of DMPS measurements, so for consistency, the diameter range 8 – 450 nm, separated into 28 logarithmically spaced size bins was selected for this study. Temperature was recorded every minute, with Pt100 sensors.

Table 1: Measurement resolution and availability of data recorded at Pallas and Värriö research stations, used in this study

| Site | Measurement | Time resolution | Time frame used in study |
|---|---|---|---|
| Pallas | Interstitial aerosol size distribution | 5.5 min | 01/2005 – 12/2020 |
| Pallas | Total Air aerosol size distribution | 5.5 min | 08/2005 – 12/2020 |
| Pallas | Visibility | 1 min | 01/2005 – 12/2020 |
| Pallas | Temperature | 1 min | 01/2005 – 12/2020 |
| Värriö | Total Air aerosol size distribution | 10 min | 01/1998 – 12/2021 |
| Värriö | Temperature | 1 min | 01/1998 – 12/2021 |

## 2.3 CLOUD ACTIVATION PARAMETERIZATION

### 2.3.1 DATA PROCESSING

Hourly median values of both the total and interstitial DMPS data at Pallas were calculated. The period of 2008 – 2014 was selected as the training period, and this dataset was used in the development of the parameterization. Hours when the visibility was less than 500 m were classified as cloudy, and this corresponded to 17% of all available data.

Such periods were used in the calculation of the size dependant activated fraction ($A_F(Dp)$), defining the number fraction of aerosol particles that have formed a cloud droplet (Eq. 1).

$$A_F(Dp) = \frac{\frac{dN_{total}(Dp)}{dlogDp} - \frac{dN_{interstitial}(Dp)}{dlogDp}}{\frac{dN_{total}(Dp)}{dlogDp}}$$

https://doi.org/10.5194/egusphere-2026-5001
Preprint. Discussion started: 11 September 2026


(1)

The calculation of the activated fraction at each size bin diameter measured by the DMPS system enabled the assembly of activated fraction curves, that overall, demonstrate expected shapes (Fig. 2); following a sigmoidal shape starting with approximately null activation at small diameters and reaching a plateau generally approaching one at larger diameters. However, some curves appeared anomalous, and data refinement was conducted, based on values that are physically reasonable but still account for measurement noise. The activated fraction curves defined by the following criteria were removed:

Criteria 1: The mean activated fraction value of the four largest size channels was less than 0.7

Criteria 2: Any activated fraction value exceeded 1.2

Criteria 3: Any activated fraction value **above** 200 nm was below -1

Criteria 4: Any activated fraction value **below** 200 nm was below -2

A sensitivity analysis for the selection of activation curve limits used in each of the above-stated criteria is presented in the Supplementary material.

Activated fraction curves carried forward for the development of the cloud activation parameterization were fitted using the Gompertz function (Eq. 2) (Gompertz, 1825) using the minimization of the sum of squared errors approach. Standard errors used in the fitting were calculated from the standard deviation of the hourly averaged DMPS data using error propagation methodology. The diameter at which 50% of aerosol particles are activated into cloud droplets is called $D_{50}$. This is a central variable utilized in this work. From the Gompertz fit to the activated fraction data (See example in Figure 2), hourly $D_{50}$ values were obtained from determining the diameter corresponding to 50% of the activation curve plateau height.

(2)

$$A_f(Dp) = a \,.\, e^{\left(-e^{\left(-b\left(D_p - c\right)\right)}\right)}$$

https://doi.org/10.5194/egusphere-2026-5001
Preprint. Discussion started: 11 September 2026


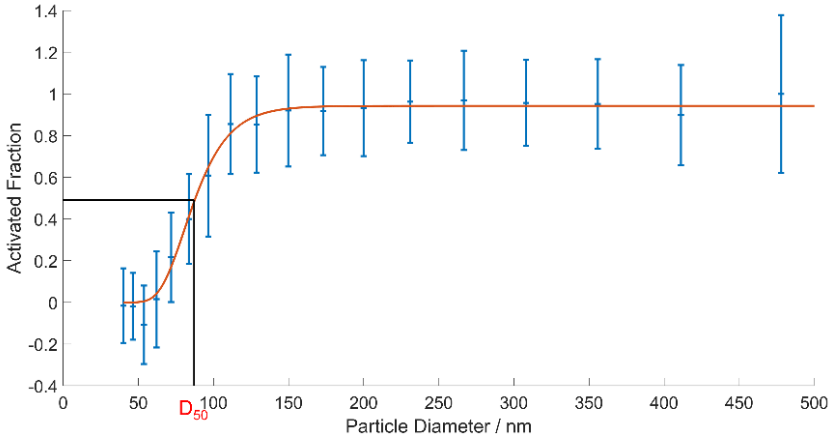


Figure 2: Example Gompertz curve function fitted to activation fraction data. Blue lines represent the activated fraction value with standard error. The red line represents the Gompertz fit. $D_{50}$ = diameter at which 50% of aerosol particles are activated.

The determined $D_{50}$ values were classified by two selected variables that can be considered as drivers of aerosol chemical composition: air temperature and air mass origin. Classification based on air temperature was chosen due to the direct relationship between temperature and aerosol organic loading (Yli-Juuti et al., 2021). Air mass origin provides an indication of the type and strength of natural and anthropogenic aerosol emissions, that the air arriving at the measurement station has been exposed to. This has been suggested to correlate with the chemical composition of the particles (Ovadnevaite et al., 2014; Kivekäs et al., 2009; Petäjä et al., 2022). Consequently, the variability in the chemical composition affects aerosol hygroscopicity (Hong et al., 2014), and hence the ability of the particles to activate into a cloud droplet ($D_{50}$ value).

The determined $D_{50}$ values were first grouped into six different temperature classes ranging from -15 to 15 °C separated by 5 °C intervals. The $D_{50}$ values separated by temperature class were further classified by air mass sectors based on a backward trajectory calculation. The trajectories were calculated using the Hybrid Single-Particle Lagrangian Integrated Trajectory (HYSPLIT) model (Stein et al., 2015). Seventy-two-hour backward trajectories were calculated, arriving at 100 m a.g.l. at Pallas every 1 hr for the period 2008–2014. Three different air mass sectors were selected to be applied to the CCN activation parameterization: Arctic, East and West as shown in Figure 3. The trajectories were assigned one of the three overall sectors based on the sector that the trajectory spent the most time in. The sector selection was based on typical air masses which both Pallas and Värriö experience (Asmi et al., 2011), and simplicity to support the creation of a robust cloud droplet activation scheme.

https://doi.org/10.5194/egusphere-2026-5001
Preprint. Discussion started: 11 September 2026


Separation of the $D_{50}$ values by six temperature classes and three air mass sectors forms a look-up table of 18 median $D_{50}$ values (Table S3) that forms the basis of the parameterization. This classification approach enables simple and logical applicability of the cloud activation parameterization. A sensitivity analysis for the choice of the sector bounds is presented in the Supplementary material.

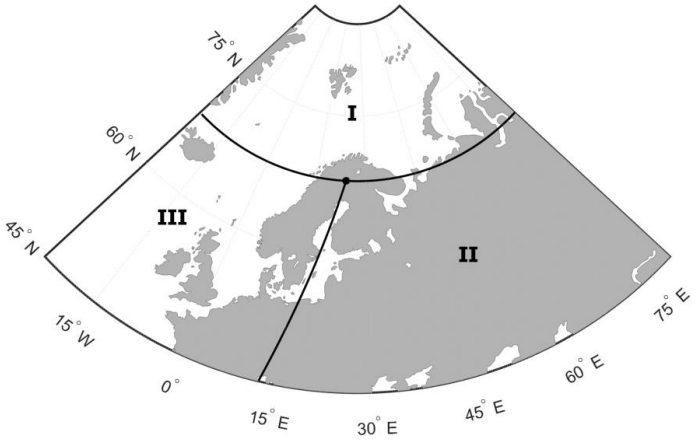


Figure 3: Map of air mass sectors used to classify trajectories arriving at Pallas (location shown as central point): I (Arctic), II (East), and III (West)

### 2.3.2 APPLICATION OF THE CLOUD ACTIVATION PARAMETERIZATION

The concentration of CCN ($N_{CCN}$) in the parameterization was obtained from the integration of hourly averaged total particle number size distribution of particles larger than the $D_{50}$ value (See Fig.4 and Eq. 3). The relevant $D_{50}$ value was found in the look-up table (Table S3) based on the combination of temperature and air mass origin classification. Interpolation of the size distribution data was necessary to provide increased resolution and enable more accurate integration around the desired $D_{50}$ value.

$$N_{CCN} = \int_{D_{50}}^{\infty} n(logD_p) dlogD_p \quad (3)$$

https://doi.org/10.5194/egusphere-2026-5001
Preprint. Discussion started: 11 September 2026


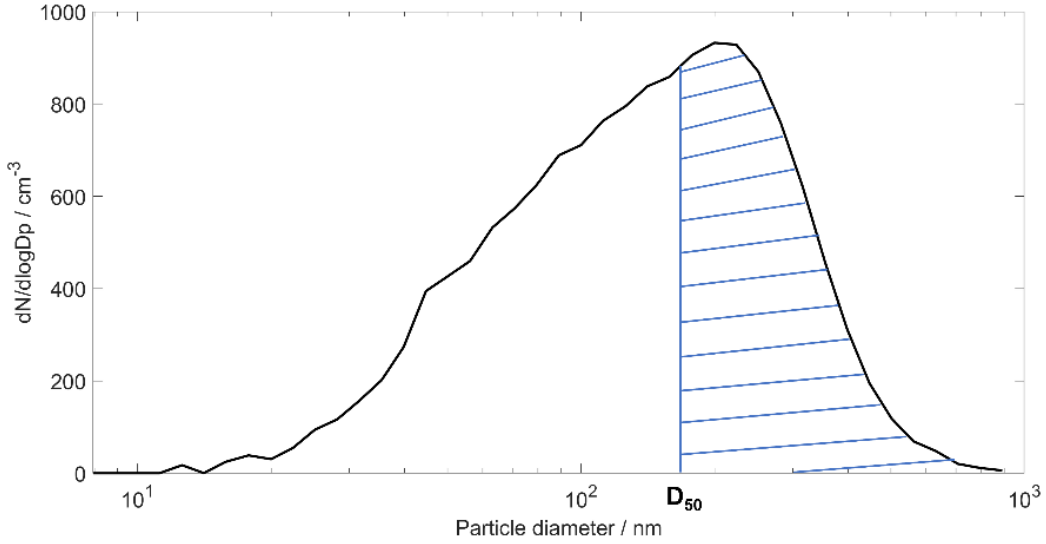


Figure 4: Integration of particle number size distribution data to obtain predicted $N_{CCN}$

At Pallas, the parameterization was applied to the aerosol size distribution data from 2005 to 2007 and from 2015 to 2020, i.e. outside of the parameterization training period. This provided a continuous CCN dataset for the years 2005-2020, that would be consistent with that from Värriö, see below.

For Värriö, the same temperature classification system was used as developed at Pallas. Trajectory analysis was conducted in a similar way to that at Pallas, but Värriö was now selected as the central point for trajectory arrival. The most significant difference to Pallas is that central Finland is now included in the West sector. Eq. 3 was then utilized for the Värriö aerosol size distribution data, resulting in CCN- concentrations for the period 1997 – 2021. The approach rests on the assumption that both Pallas and Värriö reside in a similar sub-Arctic environment, and that the air mass sector definitions are robust enough to assume similar chemistry in the defined incoming air mass sectors at both sites.

## 2.4 GLOBAL CLIMATE MODEL

The long-term observational data from this study provide a chance to evaluate how well a model captures the aerosol processes at a station over the years. EC-Earth3 AerChem is an earth system model which couples the Integrated Forecasting System (IFS) meteorological model with Tracer Model Version 5, Massively Parallel version (TM5), a component to simulate aerosols and atmospheric

https://doi.org/10.5194/egusphere-2026-5001
Preprint. Discussion started: 11 September 2026


chemistry (van Noije et al. 2021). The aerosol components represented in TM5 include sulphate (SO4), black carbon (BC), organic aerosols (OA), sea salt, and mineral dust. These are described by the modal aerosol microphysical scheme M7 (Vignati et al. 2004) as described in Stier et al. 2005, which consists of four water-soluble modes (nucleation, Aitken, accumulation, and coarse) and three insoluble modes (Aitken, accumulation, and coarse). In Bergman et al. 2022 the TM5 model was further developed to improve the representation of Secondary Organic Aerosols (SOA). For the determination of CCN- concentrations, EC-Earth3 calculates the critical dry particle diameter using Köhler theory.

Using the model, 6 ensemble runs were created, producing output from 1987 to 2015 as monthly average values. The simulations were run at horizontal resolution of 0.678 degree by 0.678 degree and a vertical resolution of 92 sigma levels. An ensemble mean of the dataset was obtained using the ensemble mean tool from Climate Data Operators (Schulzweida 2023) and the point corresponding to the Pallas and Värriö stations were obtained using nearest neighbour interpolation. A comparable dataset from the observations was created by calculating the monthly mean from the available datapoints. We used CCN at 0.2% and 1.0% supersaturation for comparison with the measured values. In an earlier case study at the Pallas station during autumn (Anttila et al. 2009), the critical supersaturation based on observations was estimated to vary between 0.18 - 0.26.

For additional calculations of representative aerosol size distributions, we ran simulations using TM5 only, from January 2019 to September 2020, with 9 months of the run considered as spin-up.

## 3 RESULTS AND DISCUSSION

### 3.1 AEROSOL SIZE DISTRIBUTIONS AND TRENDS

The aerosol size distribution is a governing factor for cloud condensation nuclei concentrations (Dusek et al., 2006). Therefore, we first look at the basic features of aerosol size distributions observed at Pallas and Värriö during the study period. For simplicity, we have segregated the size distributions into three modes, namely the nucleation mode ($D_p$ < 20 nm), the Aitken mode (20 nm < $D_p$ < 100 nm), and the accumulation mode ($D_p$ > 100 nm). The size ranges for these modes are the same as for an earlier trend analysis for both stations (Leinonen et al. 2022).

The aerosol concentrations at Pallas and Värriö were very similar, with average annual concentrations about 860 # /cm$^3$ at Pallas and 790 # /cm$^3$ at Värriö (Table 2). In the context of cloud formation, the Aitken- and accumulation mode particles are more relevant, although the nucleation mode particles have the potential to grow into CCN- active sizes as well. At both locations, the Aitken mode dominates the average annual aerosol size distribution, with over 50 % of particles residing in this size range.

https://doi.org/10.5194/egusphere-2026-5001
Preprint. Discussion started: 11 September 2026


Table 2. Annual average (N) and standard deviation, with annual trend (dN), for the nucleation mode ($D_p$ < 20 nm), the Aitken mode (20 nm < $D_p$ < 100 nm), and the accumulation mode ($D_p$ > 100 nm) for Pallas 2005-2020 and Värriö 1998-2021. Statistically significant trends (p<0.05) have been marked with an asterisk.

| | $N_{nuc}$ #/cm$^3$ | $dN_{Nuc}$ #/cm$^3$/year | $N_{Ait}$ #/cm$^3$ | $dN_{Ait}$ #/cm$^3$/year | $N_{Acc}$ #/cm$^3$ | $dN_{Acc}$ #/cm$^3$/year | $N_{Tot}$ #/cm$^3$ | $dN_{Tot}$ #/cm$^3$/year |
|---|---|---|---|---|---|---|---|---|
| Pallas avg. | 158 | 3.9 | 468 | -9.1* | 228 | -8.8* | 863 | -12.7* |
| st.dev. | 42 | | 60 | | 64 | | 103 | |
| Värriö avg. | 130 | 0.6 | 413 | -4.3* | 244 | -5.4* | 791 | -7.6 |
| st.dev. | 19 | | 61 | | 51 | | 108 | |

The long- term concentration measurements reveal a decreasing trend at both stations. At Pallas, total concentrations have decreased at a rate of about 13 # /cm$^3$ / year (p=0.0045), and at Värriö at a rate of about 8 # /cm$^3$ / year (p=0.087). This decrease is most pronounced, and statistically significant, in the Aitken and accumulation modes, with the nucleation mode showing an increasing, albeit statistically insignificant, trend.

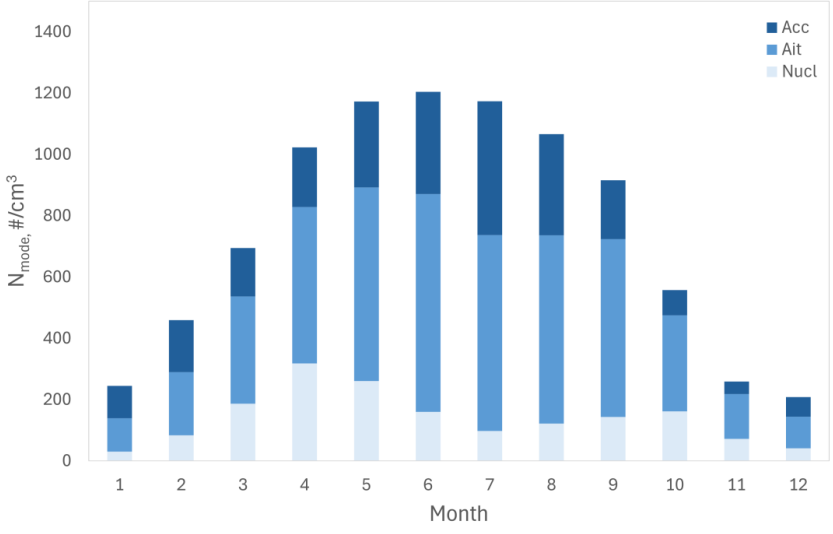


a)

https://doi.org/10.5194/egusphere-2026-5001
Preprint. Discussion started: 11 September 2026


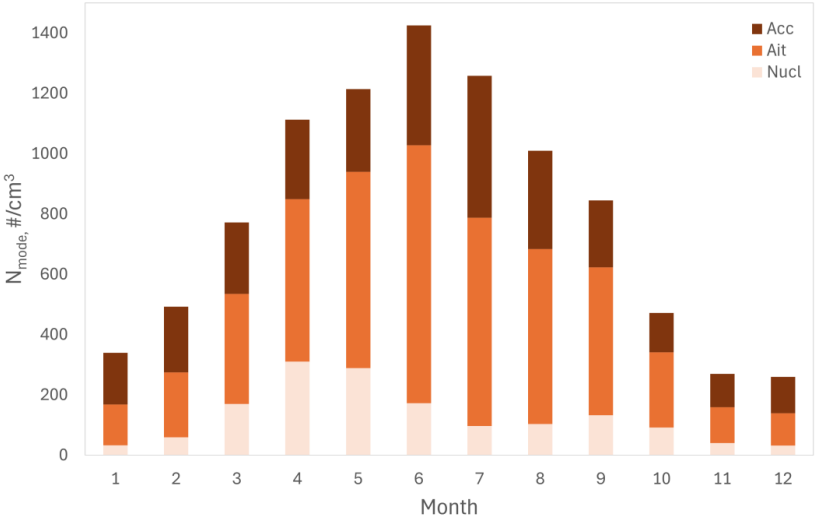


b)

Figure 5. Monthly variation of average accumulation ($D_p$ > 100 nm)-, Aitken- (20 nm < $D_p$ < 100), and nucleation- ($D_p$ < 20 nm) mode particle concentrations at a) Pallas during 2005-2020 and b) Värriö during 1998-2021.

Both stations have a pronounced seasonal variation in their aerosol size distribution (Figure 5). The highest total concentrations were found in summer, with a maximum monthly average concentration around 1220 #/cm$^3$ at Pallas and 1420 #/cm$^3$ at Värriö in June. The lowest monthly concentrations occurred in December, when the monthly average particle concentration was 210 # / cm$^3$ at Pallas and 260 # / cm$^3$ at Värriö. In the autumn, the concentrations at Pallas were slightly higher than at Värriö. The highly variable seasonal size distributions reflect the remoteness of both stations from anthropogenic aerosol sources. During summer, natural emissions dominate, while during winter, when natural activity is low, aerosol is mostly long-range-transported.

## 3.2 AEROSOL ACTIVATION AND $D_{50}$ VALUES

### 3.2.1 OBSERVED $D_{50}$ VALUES AT PALLAS

The aerosol activated fractions for occasions when the station was inside a cloud at Pallas, were calculated using Eq. 1 as described in section 2.3.1. Figure 6 presents a time-series of $D_{50}$ values as obtained from the fitting procedure (Eq. 2). The median $D_{50}$ value was 105 nm, and the lower and upper quartile $D_{50}$ values were 84 and 133 nm, respectively. Overall, there is considerable variability

https://doi.org/10.5194/egusphere-2026-5001
Preprint. Discussion started: 11 September 2026


in the $D_{50}$ values, particularly at the upper range. This may be attributed to the non-constant supersaturation of the clouds as well as variation in the CCN chemical composition.

Previous studies at Pallas that had derived $D_{50}$ values for shorter time periods, are in reasonable agreement with the presented observations. Komppula et al. (2005) reported $D_{50}$ values in the range of 50 – 128 nm, while Anttila et al. (2009) reported a range of 88 – 215 nm. Both of these observation periods were limited to autumn. Reported $D_{50}$ values from other stations tend to lie in the range of 100 – 200 nm (Väisänen et al., 2016, Henning et al., 2002, and references therein).

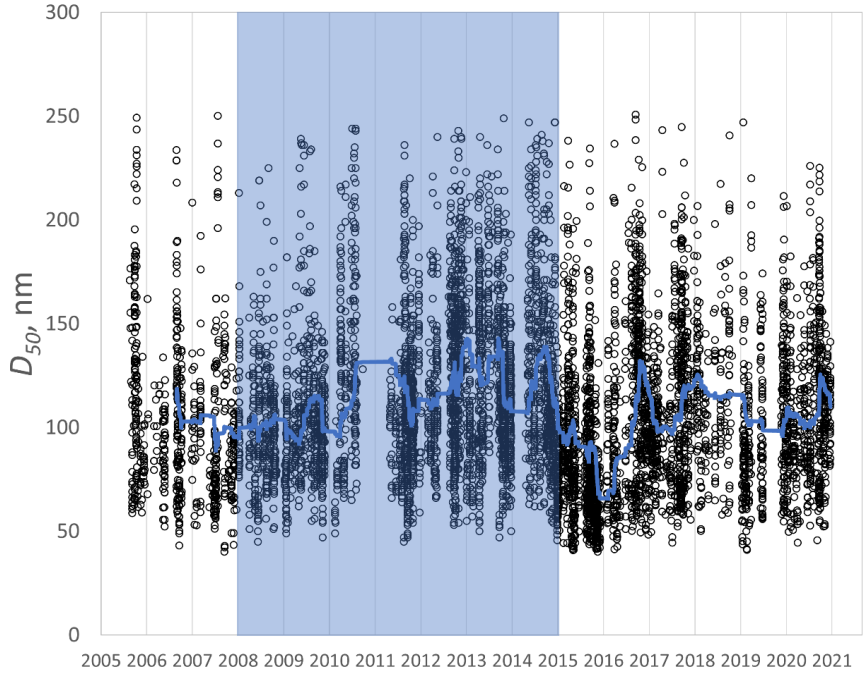


Figure 6: 1h- average diameter of the 50% cloud activated aerosol population ($D_{50}$) derived from the difference between the total and interstitial aerosol populations at Pallas. The solid line is 10-day running mean, and the training period for CCN- parameterization is shaded in blue.

In Figure 7, the seasonal variation of $D_{50}$ is shown as monthly distributions. Overall, the median and mean $D_{50}$ values are in the 100 – 125 nm range with only a weak seasonal variation. In general, low $D_{50}$ values (the 10$^{th}$ percentile value) can be seen throughout the year, while high values ($D_{50}$ > 175 nm) were not observed during winter.

https://doi.org/10.5194/egusphere-2026-5001
Preprint. Discussion started: 11 September 2026


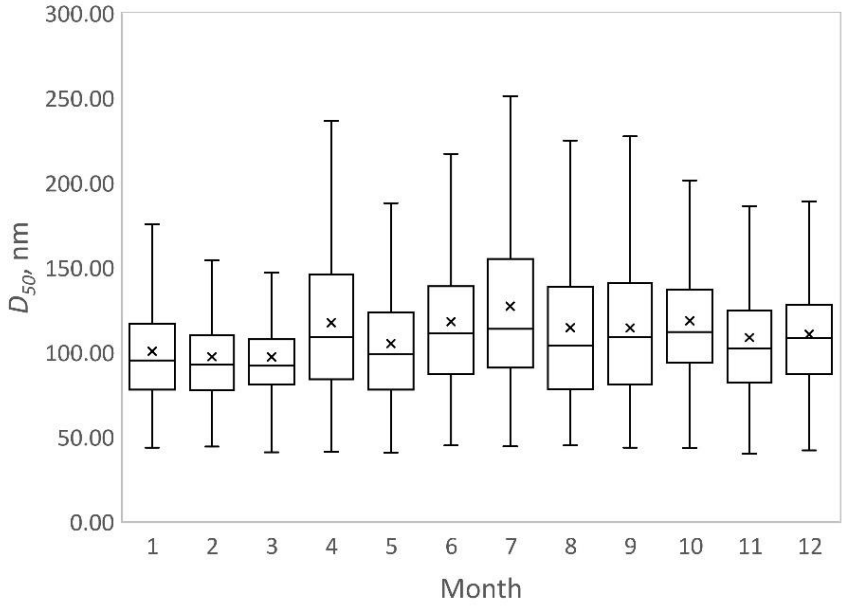


Figure 7. Monthly diameter of the 50% cloud activated aerosol population ($D_{50}$) at Pallas during 2005 – 2020. Box plot shows the 10th, 25th, median, 7th and 90th percentiles, while crosses denote the monthly average.

The greatest fraction of the cloud periods occurred during autumn and continued through to winter, concurrent with previous studies at Pallas based on shorter study periods (Jaatinen et al., 2014; Anttila et al., 2012). During this time of the year in the Northern Hemisphere, the sun's radiation hits the surface of the Earth, 1) at a shallower angle resulting in less surface heating; 2) for shorter periods of time leading to colder air temperature. Subsequently, this increases the likelihood of supersaturated water vapour in the air.

### 3.2.2 $D_{50}$ PARAMETERIZATION

The $D_{50}$ values presented in section 3.2.1 were the basis for the CCN parameterization. The parameterization training set comprised of data measured from 01/2008 to 12/2014 and was classified by two variables: air temperature and air mass origin, as first introduced in section 2.3.1. The remaining data, from 08/2005 to 12/2007, and from 01/2015 to 12/2020 was used to evaluate the parameterization performance at Pallas (See section 3.4.1).

https://doi.org/10.5194/egusphere-2026-5001
Preprint. Discussion started: 11 September 2026


Figures 8a and 8b display the median $D_{50}$ values based on the 6 temperature and 3 air mass origin classifications, respectively. The look-up table of these values, alongside a more detailed statistical distribution can be found in the Supplementary data, Table S3. The median $D_{50}$ values form the centre of the cloud activation parameterization.

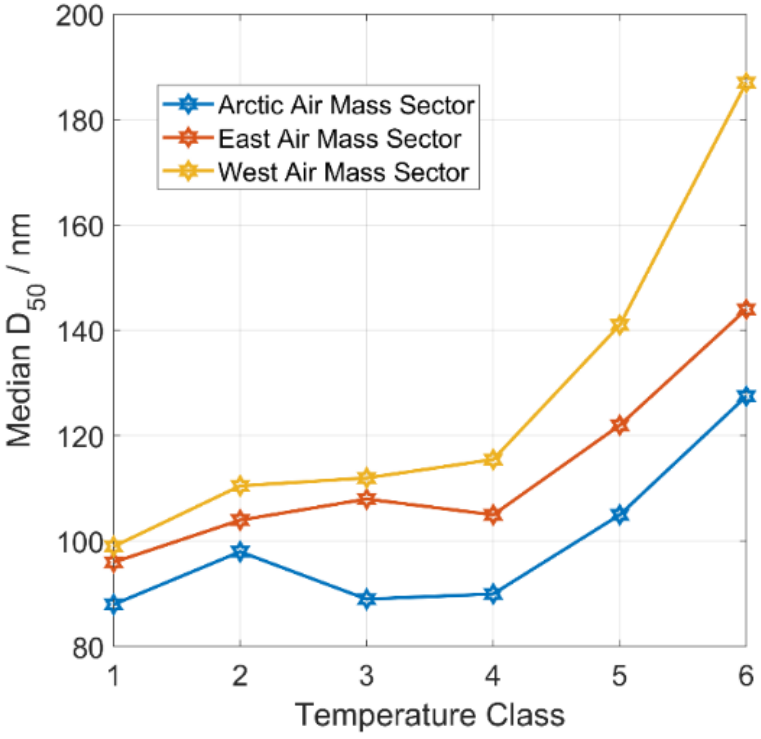


a)

https://doi.org/10.5194/egusphere-2026-5001
Preprint. Discussion started: 11 September 2026


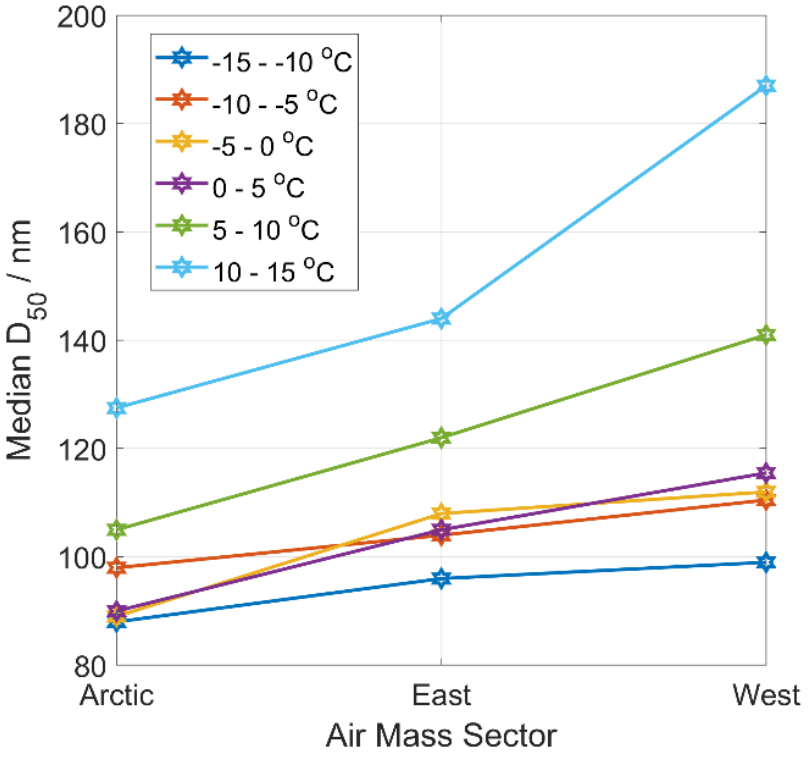


b)

Figure 8. Median $D_{50}$ values obtained from the fitted activated fraction data derived from the total and interstitial aerosol concentrations during cloudy periods at Pallas (2008 – 2014), calculated based on air temperature and air mass origin classifications. a) as a function of temperature classification: Class 1(-15 - -10 °C), 2(-10 - -5 °C), 3(-5 – 0 °C), 4(0 – 5 °C), 5(5 – 10 °C), 6(10 – 15 °C).; b) as a function of air mass sector.

Almost consistently, the median $D_{50}$ values increase as the temperature class increases in each air mass sector (Figure 8a). This increase may be attributed to potential increases in the relative contribution of organics to the aerosol composition. With increased temperatures, it has been shown, that emissions of biogenic volatile organic compounds (BVOCs) from vegetation increase (Kesselmeier and Staudt, 1999). Recent investigations at Hyytiälä SMEAR II station, a site with surroundings relatively comparable to that of Pallas, demonstrated that the organic loading of an aerosol particle increased directly with an increase in temperature (Yli-Juuti et al., 2021). This, in turn, would be expected to decrease the hygroscopicity of the aerosol particle (Hong et al., 2014), hence, increasing the diameter at which the particle can activate into a cloud droplet. Temperature has also been found

https://doi.org/10.5194/egusphere-2026-5001
Preprint. Discussion started: 11 September 2026


to correlate well with BVOC emissions also at Pallas (Hellén et al., 2020). It is notable that during wintertime, the temperature dependence is nearly flat, supporting the hypothesis that BVOC-emissions are the main driver of the observed temperature dependence.

Observing the $D_{50}$ trends by air mass origin in Figure 8b, consistently for each temperature class, $D_{50}$ values in the Arctic sector are the lowest, they increase in the East sector, and the largest values are observed in the West sector. This is likely to be attributed to differences in the chemical composition of the aerosol from different source regions. Air masses arriving at Pallas from the Arctic come directly over the marine environment where aerosol sources are mainly composed of primary sea spray and secondary sulphate (Leck et al., 2002; Sanchez et al., 2018). The subsequent hygroscopic nature of marine aerosols provides plausible rationalisation for the lowest observed $D_{50}$ values in the Arctic sector. For the Western and Eastern sector, the most notable difference is the potential for the air masses to spend time over land. Studies have demonstrated that as an air mass spends time over boreal forest regions, the organic aerosol mass concentration increases linearly with time over land (Petäjä et al., 2022). This would reduce the hygroscopicity of the aerosol. Comparing the East and West sector $D_{50}$ values, the Eastern sector hosts large industries in Eastern Continental Europe and the Kola peninsula, emitting sulphate-based, and therefore more hygroscopic, aerosol particles (Virkkula et al., 1997, Sipilä et al., 2021).

### 3.3 CCN- CONCENTRATIONS AT PALLAS AND VÄRRIÖ

CCN concentrations over time were obtained by applying the CCN- parameterization (Eq. 3 with $D_{50}$-values from the look-up Table S3) to the long-term DMPS- measurements at both sites. At Pallas, to maximize the time series length while ensuring the homogeneity of the dataset, the cloud screened, interstitial aerosol size distribution data were used. The data covered 01/2005 – 12/2020 for Pallas and 12/1997-11/2021 for Värriö, making these one of the longest CCN- time series reported from sub-Arctic regions.

#### 3.3.1 LONG TERM VARIATION

The average annual CCN concentrations at Pallas and Värriö were approximately 140 ± 40 # /cm$^3$ (median 90 # /cm$^3$) and 170 ± 50 # /cm$^3$ (median 130 # /cm$^3$), respectively. The seasonal variation of the CCN concentrations was high at both stations, with 1-h average CCN concentrations spanning from less than 1 to more than 1000 # / cm$^3$, as seen in Figure 9. Supplementary Figure S1 shows the statistical distribution of CCN concentrations at both stations. It is notable that even though total

https://doi.org/10.5194/egusphere-2026-5001
Preprint. Discussion started: 11 September 2026


aerosol concentrations at Pallas were slightly higher than at Värriö (see Table 2), the CCN concentrations were lower at Pallas. This is because at Värriö, the accumulation mode concentrations were higher, and these particles activate more readily. However, the differences are within statistical variation.

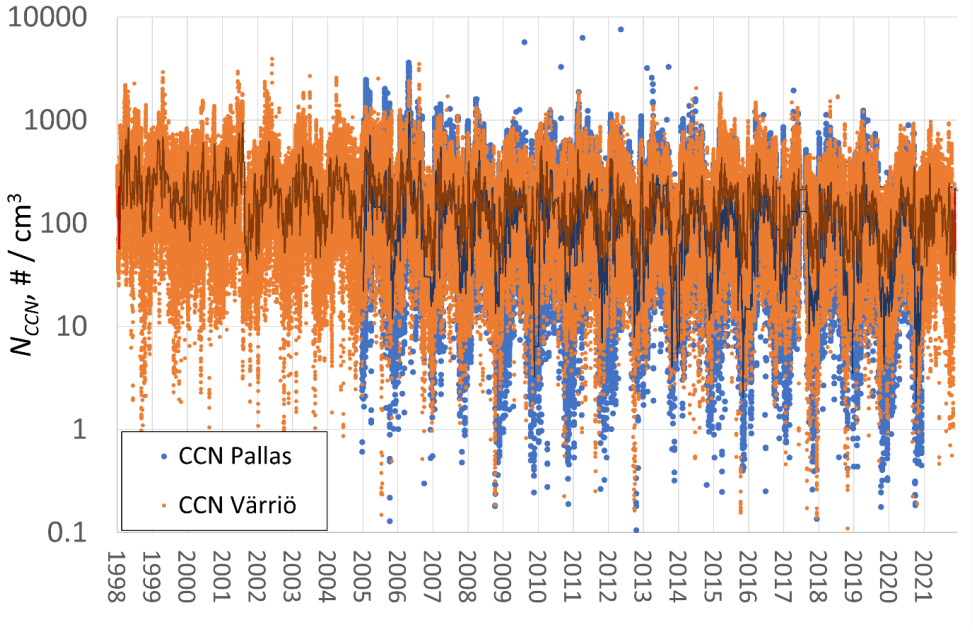


Figure 9. Timeline of 1h average CCN concentrations with a 10-day running mean in Pallas (blue) and Värriö (red), based on CCN parameterization.

A trend analysis of the long-term CCN concentration reveals a clear, statistically significant decreasing trend for both sites, see Figure 10. At Pallas, the median annual concentration has decreased steadily at a rate of -2.5 CCN /cm$^3$ / year, and at Värriö at a rate of -4.2 CCN /cm$^3$ / year. For the same period as in Pallas, the trend in Värriö is about -3.3 CCN / cm$^3$ /year.

https://doi.org/10.5194/egusphere-2026-5001
Preprint. Discussion started: 11 September 2026


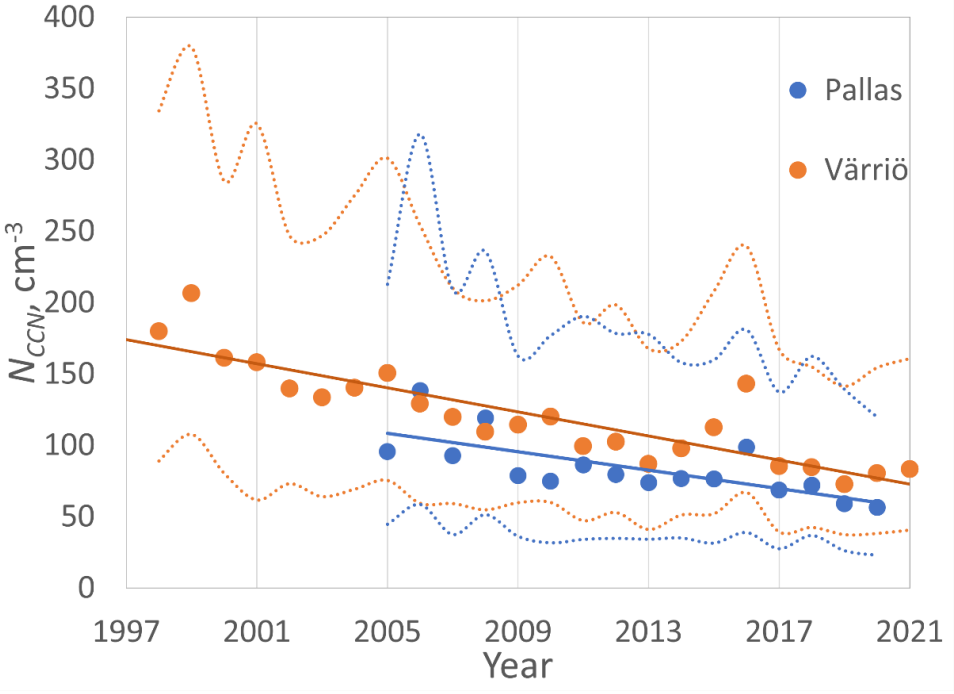


Figure 10. Annual trend of CCN- concentrations at Pallas during 2005 – 2020 (blue) and Värriö during 1998 – 2021 (red). Markers are annual median concentrations, solid lines are linear fits to the medians, and dashed lines indicate the annual upper and lower quartiles.

Monthly long-term data were also analyzed to find out how different months contribute to the observed long-term trend. At Värriö, all months except July, August and September show a statistically significant decreasing long-term trend, with strongest trends in February, March and April with slopes of -8.3, -8.8 and -6.8 CCN / cm$^3$ / year, respectively. Meanwhile at Pallas, February and March are the only months to show statistically decreasing trends at -8.0 and -7.6 CCN / cm$^3$ / year, respectively; and contrarily, the summer month of July shows a positive, however a non-significant trend of +5.3 CCN / cm$^3$ / year. This highlights that the decreasing trend was mostly due to a decrease in anthropogenic aerosols (Arctic Haze), while natural aerosols can play even an opposite role.

### 3.3.2 SEASONAL VARIATION

The CCN concentrations show a distinctive seasonal variation for both sites, see Figure 11. At Pallas high CCN concentrations were observed from May to August, and low concentrations from October

https://doi.org/10.5194/egusphere-2026-5001
Preprint. Discussion started: 11 September 2026


to January. At Värriö, highest CCN concentrations were additionally observed from February to April, and concentrations were lowest from October to December. At Värriö, the Arctic Haze phenomenon appeared stronger (most likely due to emissions from the Kola region), leading to the highest CCN concentrations in the first quarter of the year.

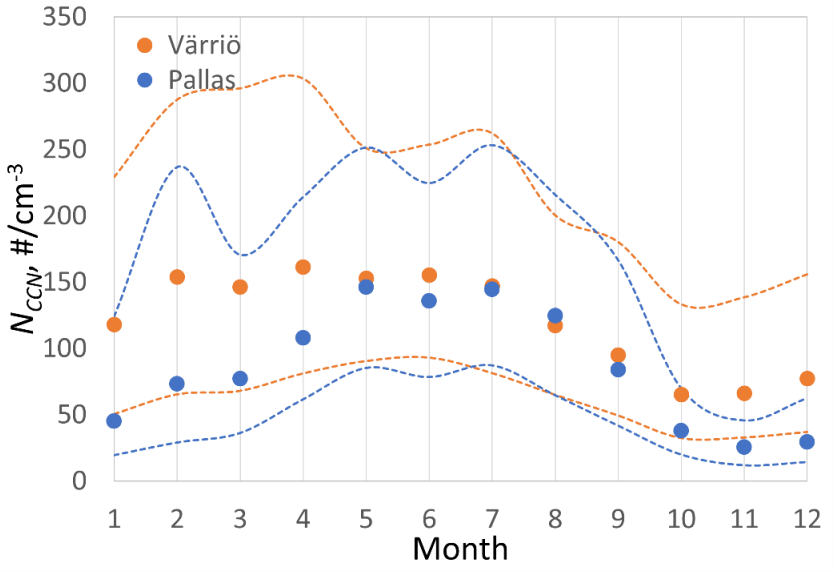


Figure 11. Seasonal variation of CCN- concentration at Värriö during 1998 – 2021 (red) and Pallas during 2005 – 2020 (blue). Solid lines with markers are median values, while dashed lines indicate the upper and lower quartiles.

Figure 12 illustrates how particles in different size modes activated into cloud droplets during different seasons. Assuming that largest particles activate first, the shaded area of bars in Figure 13 act as CCN. At both sites during winter (from November to February), the whole accumulation mode, comprising 30 to 50 % of all particles, activated into cloud droplets. However, in March, April and May, the fraction of accumulation mode particles acting as CCN decreased. This reaches a minimum in June and July, when only about 15 % of all particles activated into cloud droplets. From August to October a larger fraction of accumulation mode particles began to act as CCN again. The seasonal variation in the fraction of aerosol particles forming cloud droplets illustrates the role of organic aerosol in cloud formation. Even though the number of aerosol particles increases in the summer due to secondary organic aerosol formation, the aerosol hygroscopicity decreases, which in turn increases the $D_{50}$ activation diameter.

https://doi.org/10.5194/egusphere-2026-5001
Preprint. Discussion started: 11 September 2026


Another possible explanation for the summertime behavior is that the aerosol activation conditions shift from the aerosol-limited cloud activation regime to the transitional regime, and a decreasing supersaturation hinders cloud formation. To inspect this, we utilized the same updraft velocity ($\sigma_w$) measurements at Pallas as presented by Virtanen et al. (2025). While monthly averages correspond to conditions being in aerosol-limited regime ($\sigma_w / N_{tot} < 10^{-3}$ m/s cm$^3$) (Reutter et al., 2009) throughout the year, we note that the monthly 25$^{th}$ percentile values of $\sigma_w$ are in the range of 0.1 – 0.3 m/s during April – September. Considering the elevated aerosol concentrations at Pallas and Värriö during these months, these values correspond to conditions shifting just to the transitional regime. Therefore, it is plausible that limited supersaturation had partly caused the observed ineffective aerosol activation during summer.

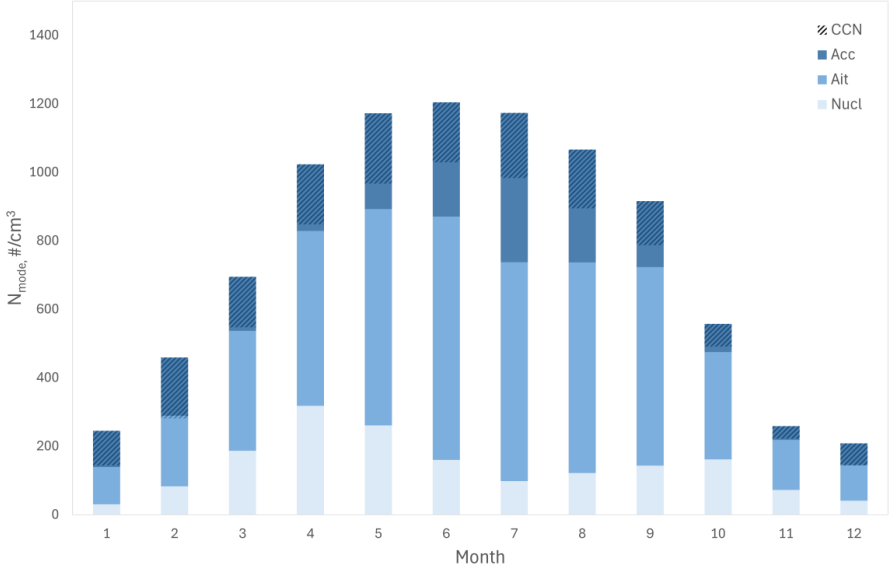


a)

https://doi.org/10.5194/egusphere-2026-5001
Preprint. Discussion started: 11 September 2026


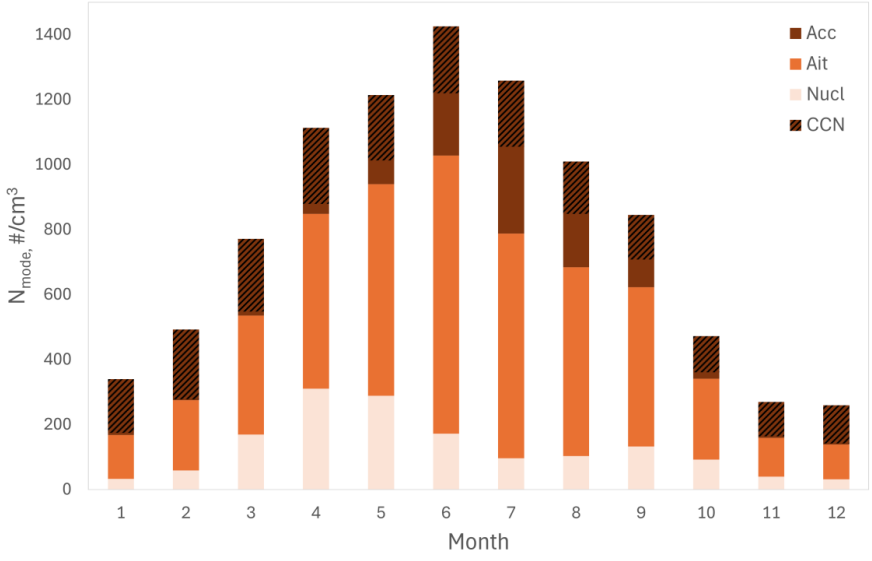


b)

Figure 12. Monthly average CCN- forming potential of particle size distribution modes. Color bars denote the fractional contribution of the different particle modes to the total particle concentration (See Figure 5.). The shaded bar areas indicate particles acting as CCN. a) Pallas, b) Värriö.

What should also be kept in mind is that the $D_{50}$- activation diameter has a wide statistical distribution. It would be a misinterpretation to conclude that Aitken mode particles did not activate into cloud droplets. In fact, particles from the Aitken mode activated throughout the year (Fig. 7). However, it is clear that particle size distribution plays a significant role in cloud formation on average, and that an increase in larger particles will have a more effective cloud formation potential compared to smaller particles.

### 3.4. COMPARISON TO GLOBAL CLIMATE MODEL RESULTS

One of the motivations of the study was to provide observational constraints to global climate models. Utilizing data from two stations with a distance similar to global climate model grid cell size mitigates the uncertainty of observation representativeness. Here, we compare the observed seasonal- and long-term trends for aerosols and CCN at Pallas and Värriö to the TM5 (for aerosol size distribution) and the EC-Earth3 AerChem (for CCN) model results.

https://doi.org/10.5194/egusphere-2026-5001
Preprint. Discussion started: 11 September 2026


Figure 13 illustrates the comparison of long-term CCN concentration trends between EC-Earth3 and the observations. We utilized CCN- concentrations at pre-determined 0.2% and 1.0% supersaturations as outputs from EC-Earth3. This was chosen despite the availability of CDNC concentrations as the model takes into account the cloud cover resulting in a dataset that is not directly comparable to the observations. What can consistently be observed from both stations' data is that the modelled long term CCN concentration at 0.2% supersaturation follows closely the observed decreasing $N_d$ trend, with concentration within the variance range. This can be considered a very good estimation, given that the critical supersaturation inside the real clouds was estimated earlier (Anttila et al. 2009) to vary between 0.18 – 0.26. The probability density functions of CCN from EC-Earth3 are provided in Supplementary figure S4.

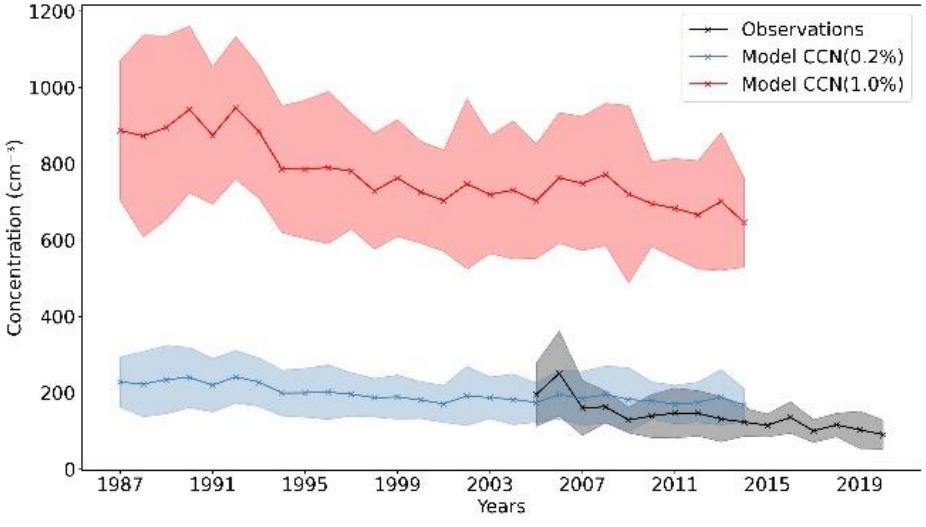


a)

https://doi.org/10.5194/egusphere-2026-5001
Preprint. Discussion started: 11 September 2026


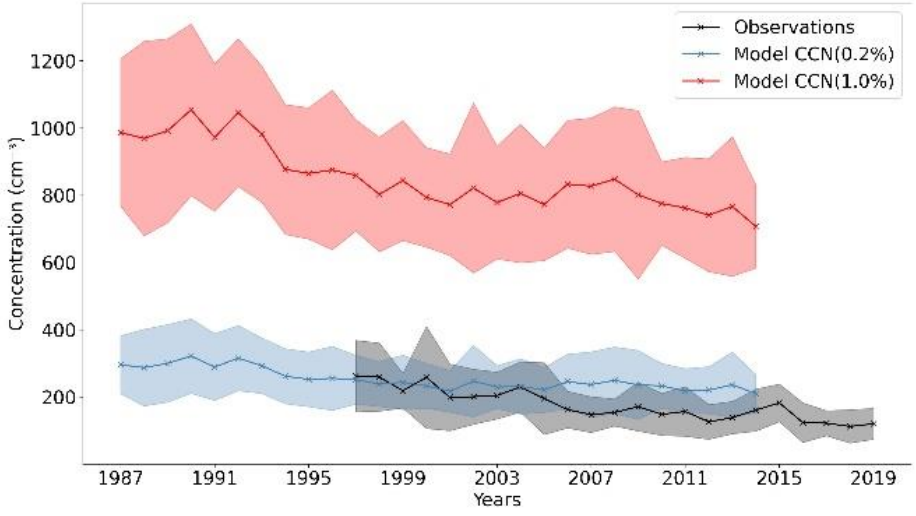


b)

Figure 13: Yearly average values of measured CCN values, modelled CCN at 0.2% and 1.0% supersaturation and modelled CDNC values. a) Pallas; b) Värriö. The shaded area represent variance.

To pinpoint reasons for possible discrepancies between the model and observations, aerosol size distributions were modelled by the TM5 model for a representative period of 10/2019-09/2020. The measured and modelled aerosol concentrations are quite similar to each other. However, there some differences in the modal concentrations, with the model overestimating nucleation mode concentrations while underestimating accumulation mode concentrations, see Table 3. As the CCN concentration is sensitive to the concentration of the accumulation mode particles, this may also decrease the amount of modelled CCN's. This is in contradiction with the slight overestimation that can be observed in Figure 13.

Table 3. The average ± standard deviation of monthly data for nucleation ($N_{Nuc}$), Aitken ($N_{Ait}$) and accumulation ($N_{Acc}$) mode particle concentrations from the measurements and TM5 from 10/2019 to 09/2020.

| | $N_{nuc}$, #/cm$^3$ | $N_{Ait}$, #/cm$^3$ | $N_{Acc}$, #/cm$^3$ | $N_{Tot}$, #/cm$^3$ |
|---|---|---|---|---|
| Pallas | | | | |
| Measured | 163±145 | 413±325 | 144±139 | 729±528 |
| TM5 | 229±235 | 331±115 | 79±17 | 638±331 |
| Värriö | | | | |

https://doi.org/10.5194/egusphere-2026-5001
Preprint. Discussion started: 11 September 2026


| | | | | |
|---|---|---|---|---|
| Measured | 151±132 | 424±337 | 189±153 | 783±559 |
| TM5 | 224±208 | 432±124 | 97±25 | 752±290 |

512

513 The climate-model-predicted seasonal variation of aerosol concentrations (Figures 14a1 and 14b1 )
514 are similar to observations (Figure 11 and 12), however with TM5 predicting maximum concentrations
515 already during May–June, rather than in July as seen in the observations. We can speculate that this
516 is caused by an underestimation of secondary aerosol formation, and/or missing growth to
517 accumulation sized particles. Furthermore, TM5 predicts relatively higher aerosol concentrations in
518 November and December compared to the measurements especially in Värriö. This propagates to the
519 estimation of CCN concentrations, which rise sharply from October to January, unlike seen in the
520 observations. The aerosol population during this period is dominated by particles transported from
521 surrounding regions. Prank et al. (2010) shows that emissions from Nikel have partly been attributed
522 to Murmansk, which is closer to the two stations considered in this study. A similar misattribution
523 could partially explain the overestimation of aerosol- and CCN concentrations.

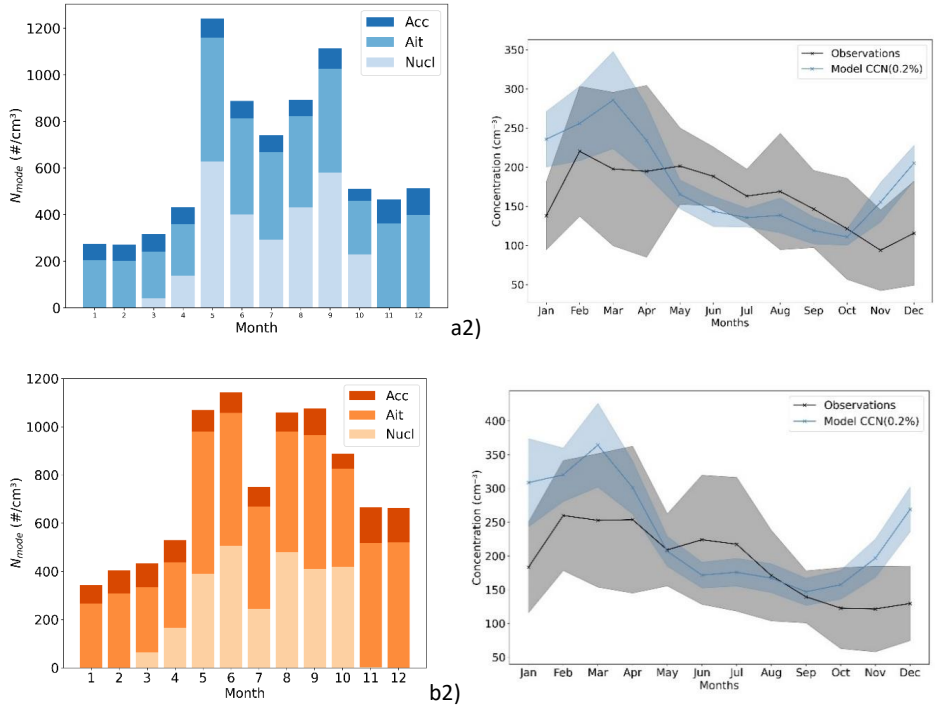


524 a1) a2)

525 b1) b2)

526 Figure 14 : Monthly average values from TM5 at a) Pallas and b) Värriö for 1) nucleation-, aitken- and
527 accumulation mode particle concentrations; and from EC-Earth3 2) for $N_{CCN}$ at SS=0.2% compared to
528 observations.

https://doi.org/10.5194/egusphere-2026-5001
Preprint. Discussion started: 11 September 2026


529

530 ### 3.5 DIAGNOSTICS OF THE CCN-PARAMETERIZATION

531 #### 3.5.1 PARAMETERIZATION PERFORMANCE EVALUATION

532 The CCN-parameterization performance was evaluated by first investigating the agreement of the $D_{50}$
533 diameters predicted by the parameterization from each trajectory/temperature-bin pairs (Table S3)
534 against $D_{50}$ determined at Pallas during in-cloud events outside of the parameterization training
535 period, i.e. from 2005 to 2007, and from 2015 to 2020. For the measurements, the total- and
536 interstitial size distribution data was used, and equations 1 and 2, including the data quality criteria,
537 were used to deduct the $D_{50}$- diameters. Figure 15 illustrates that there is reasonable agreement
538 between the measured median $D_{50}$- values and the $D_{50}$- values from the parameterization. However,
539 the distribution of the measured $D_{50}$ values was relatively broad for all individually parameterized $D_{50}$-
540 values, with the observed 25$^{th}$ percentiles being on average 23 nm lower, and the 75$^{th}$ percentiles 25
541 nm higher than the parameterized $D_{50}$- diameter. Furthermore, for the very highest $D_{50}$ class (for
542 Western airmass and 10 C°<T<15 C°), the training dataset gives a clearly higher value compared to the
543 evaluation dataset. This is likely due to the small training sample size (28 data points) for this individual
544 data bin.

https://doi.org/10.5194/egusphere-2026-5001
Preprint. Discussion started: 11 September 2026


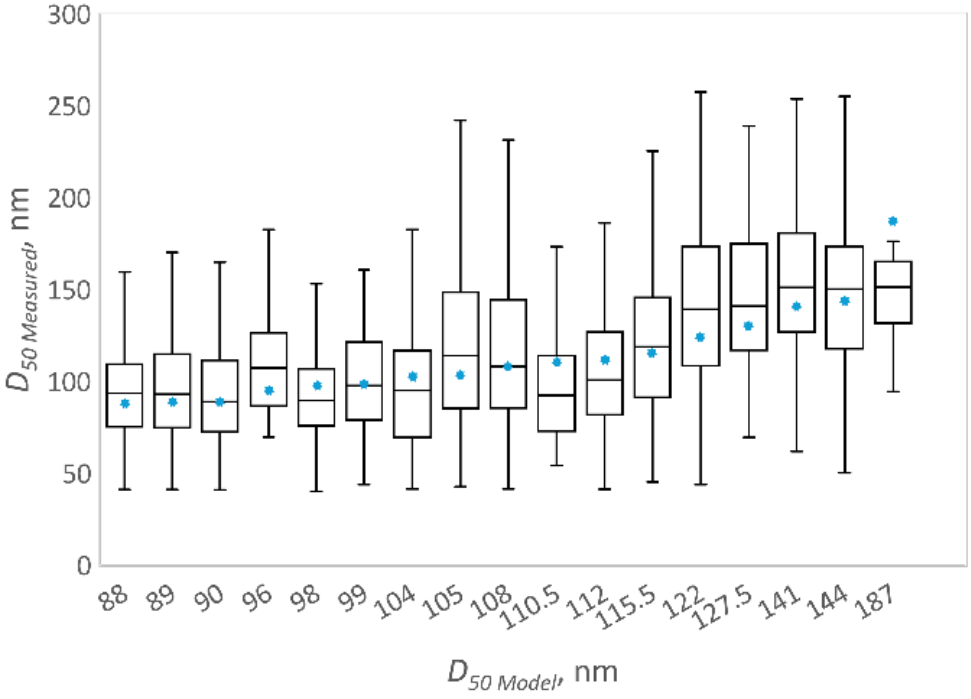


Figure 15. Statistical evaluation of the $D_{50}$ diameter median diameters derived from the parameterization. The blue stars denote to parametrized bin median values, and the box plot illustrates the corresponding measured values ($10^{th}$, $25^{th}$, $50^{th}$, $75^{th}$ and $90^{th}$ percentiles) during in-cloud events from 2005 to 2007, and from 2015 to 2020 at Pallas.

https://doi.org/10.5194/egusphere-2026-5001
Preprint. Discussion started: 11 September 2026


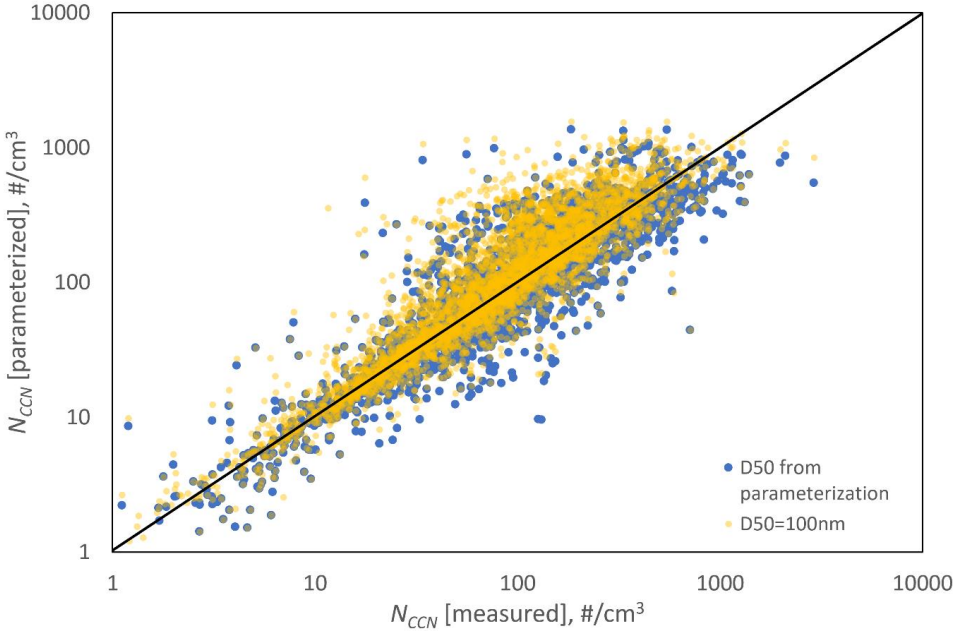


551

552 Figure 16. Comparison of the measured (using the total and interstitial DMPS set-up) vs.
553 parameterized hourly $N_{CCN}$ during in-cloud events from 2005 to 2007, and from 2015 to 2020 at Pallas.

554

555 Figure 16 displays the comparison between the measured CCN- concentrations and those from the
556 parameterization during the evaluation period. To evaluate the parameterization against in-cloud
557 measurements, now the total inlet size distribution, with eq. 3, was used as base data for the
558 parameterization. Overall, the parameterization predictions agree well with the measurements, with
559 $R^2$ = 0.83 and a slope of 0.95. We also tested how a conventional method of assuming a fixed $D_{50}$-
560 diameter compares with the parameterization approach in estimating $N_{CCN}$. Assuming a $D_{50}$= 100 nm
561 resulted in $R^2$ = 0.82, and a slope of 0.90, i.e. nearly identical to the parameterization. This highlights
562 the role of the broad statistical distribution of the individual $D_{50}$- diameter values from the
563 parameterization. While the approach is suitable for statistical tasks such as comparing against climate
564 simulations, it is less suitable for investigating individual cloud cases, as discussed in the following
565 "Parameterization limitations"- section. The largest benefit of using the parameterization approach
566 compared to using a fixed $D_{50}$ value in our study, occurs when the temperature is between 5 C˚ and 15
567 C˚, and the trajectories arrive from the East and West sectors. For these combinations $D_{50}$= 100 nm
568 would clearly be too low a value, leading to considerable overestimation of CCN concentrations.

569

https://doi.org/10.5194/egusphere-2026-5001
Preprint. Discussion started: 11 September 2026


### 3.5.2 PARAMETERIZATION LIMITATIONS

There are several sources for uncertainties when determining CCN- concentrations with the method used here. First, as the measurements are made inside a real cloud, there are fluctuations in the supersaturation. Second, the relationship of the aerosol chemical composition with air mass classification and temperature is naturally not constant. Both of these cause a distribution of $D_{50}$-diameter values (see Table S3), leading to an uncertainty in the parameterized $N_{CCN}$. Third, there are measurement errors and instrumental noise in both DMPS instruments which become amplified when being used in calculations of the activated fraction. Affirmatively, using direct measurements of the activation ratios often resulted in activation curves that were not sigmoidal, especially at low concentrations.

More strict definitions of air mass trajectory source regions, as well as utilizing updraft velocity information, could help constrain the difference between the parameterization and measured $N_{CCN}$.

## 4. SUMMARY AND CONCLUSIONS

In this study, we presented long-term CCN concentrations in the Finnish sub-Arctic, based on surface measurements at Pallastunturi- and Värriö- research stations. At Pallas, the research station is regularly inside low-level clouds, representative of large sub-Arctic stratocumulus cloud fields. Here, aerosol activation measurements between 2005 and 2020 were utilized to develop a simple parameterization of cloud activation, and to assess the performance of the parameterization. The parameterization is based on derivation of the aerosol activation diameter ($D_{50}$) during different meteorological conditions (air mass origin and temperature) and estimating the CCN- concentration from aerosol size distribution measurements. As the parameterization is based on actual aerosol activation measurements inside real clouds, supersaturation as a variable is implicitly embedded in it. This parameterization was then applied at Värriö, where aerosol size distribution measurements have been made during 1998-2021. This provided a time series of CCN concentrations which, to our knowledge, is the longest reported from the Arctic region.

The median $D_{50}$ value measured at Pallas was 105 nm, with lower and upper quartiles of 84 and 133 nm, respectively. The average annual CCN concentrations were 140 ± 40 # /cm$^3$ and 170 ± 50 # /cm$^3$ at Pallas and Värriö, respectively. According to our data, the annual average CCN- concentrations (≈$N_d$) have decreased by about 55 % during 1998-2021 at Värriö, and by about 45 % during 2005-2020 at Pallas. This was mostly due to decreases in anthropogenic aerosols, as statistically significant decrease occurred during the seasonal Arctic Haze period. McCoy et al. (2017) estimated the change of $N_d$ from the pre-industrial era to present day. They utilized a combination of remote-sensing estimates within

https://doi.org/10.5194/egusphere-2026-5001
Preprint. Discussion started: 11 September 2026


stratocumulus regions from 2001- 2013, aerosol reanalysis and Aerocom Phase II models, and found an about 2.5-3.0 times increase of $N_d$ in our study region from the pre-industrial era to present day due to human emissions (See Figure 9 in McCoy et al., 2017). If the annual decrease of $N_d$ observed in this study remains similar, it can be estimated that $N_d$ concentrations in the Finnish sub-Arctic will resemble pre-industrial levels already by the end of the current decade.

The seasonal variation of the CCN concentrations was high at both stations, and 1h- averaged CCN-concentrations spanned from less than 1 to more than 1000 #/cm$^3$. At Pallas, CCN concentrations were high from May to August, and at Värriö, the highest CCN concentrations were additionally observed from February to April. For both sites, concentrations were lowest from October to December.

The determined $D_{50}$- values imply that mostly the accumulation mode particles act as CCN, and that the particle chemistry of the accumulation mode is in a key position to affect aerosol activation. This was particularly evident in the winter and spring data, when anthropogenic aerosols dominate and most of the accumulation mode has the potential to activate into cloud droplets. However, during summer, when natural, organic aerosol dominates, on average less than 50% of the accumulation mode particles activate into cloud droplets. The low susceptibility of cloud droplet formation to aerosol concentrations during summer may partly be also due to aerosol activation moving from an aerosol limited regime to the transitional regime.

Comparison measurements to EC-Earth3 global climate model results revealed that the model was able to capture the general decreasing trend in CCN concentration, and CCN modelled at 0.2% supersaturation are close to the concentration levels of the measured CCN in real clouds. However, we find that the model is unable to capture seasonal cycle of aerosol size distributions and CCN values. We can speculate that this is due to incorrect emissions of aerosol precursors resulting in missing secondary aerosol formation, and possible misattribution of emissions from the Kola- region. The long term observations provides an opportunity to understand the long-term behaviour of CCN in the model.

Assessment of the parameterization performance provides additional insights into aerosol-cloud interactions and their measurements inside real clouds. We found that similar meteorological conditions (classified by air mass origin and temperature) resulted in a broad distribution of $D_{50}$-values. This is likely due to a fluctuating supersaturation inside real clouds and/or considerably different particle chemistry inside a single parameter class. This implies that apart from specific meteorological conditions, a pre-defined constant $D_{50}$- diameter can be an adequate choice when estimating CCN- concentrations from aerosol size distribution measurements.

https://doi.org/10.5194/egusphere-2026-5001
Preprint. Discussion started: 11 September 2026


Finally, a few words about the limitations of the study and of the developed cloud activation parameterization. When developing the parameterization, we did not exclude precipitating clouds or take the cloud phase into account. Obviously the exact CCN- parameterization cannot be extended very far beyond the presented study regions, as air mass classes and the temperature dependence of aerosol activation varies with the location. However, the principle and approach can be used at other locations as well. Given the above, the parameterization is applicable as a statistical approach for $N_{CCN}$ determination, rather than for individual cloud cases. However, our study provides a simple method for extending the estimation of CCN concentrations, if, for example, campaign-type measurements have been first been conducted to determine representative $D_{50}$ diameters.

## Author contributions

MS and APH designed the study. CGS performed the experimental CCN analysis under supervision of KN and completed the first version of the manuscript. TN performed the trajectory analysis. AC, JM and RM performed the global model simulations and analysis. CGS, APH, AV, RM and JJ discussed the results. APH edited the manuscript. All authors reviewed and approved the final version of the manuscript

## Competing interests

The authors declare that they have no known competing financial interests or personal relationships that could have appeared to influence the work reported in this paper.

## Data and code availability

The interstitial inlet aerosol number size distribution from Pallas, and aerosol size distribution from Värriö are available through the EBAS database (https://ebas.nilu.no). The meteorological data sets from Pallas (Sammaltunturi) are available at https://en.ilmatieteenlaitos.fi/download-observations, and from Värriö at https://smear.avaa.csc.fi/. The total inlet aerosol number size distribution from Pallas, the derived $D_{50}$ and CCN time series from Pallas and Värriö, and the results from the EC-Earth3 and TM5 are available at the METIS data portal (DOI:10.57707/fmi-b2share.kg4ej-9sy11). The TM5-MP is available in GitLab repository hosted by KNMI. Access can be obtained by emailing Philippe Le Sager (sager@knmi.nl). The TM5-MP used is the version developed in FORCeS project. The HYSPLIT model is available at http://ready.arl.noaa.gov/HYSPLIT.php.

https://doi.org/10.5194/egusphere-2026-5001
Preprint. Discussion started: 11 September 2026


## Acknowledgements

The authors gratefully acknowledge the technical and station staff at the Pallas Atmosphere-Ecosystem Supersite and the Värriö SMEAR I station for maintaining the long-term measurements.

## Financial support

This research has been supported by the Research Council of Finland through the ACCC Flagship and Centre of Excellence funding (grant nos. 359340, 359342, 359343, 374081, and 374082), by ACTRIS-FI 2020–2024 (grant no. 328616) supporting the Värriö station, and by the Finnish Meteorological Institute through funding from the Ministry of Transport and Communications for ACTRIS.

## References

Aalto, P., Hämeri, K., Becker, E., Weber, R., Salm, J., Mäkelä, J. M., Hoell, C., O'Dowd, C. D., Hansson, H.-C., Väkevä, M., Koponen, I. K., Buzorius, G., and Kulmala, M.: Physical characterization of aerosol particles during nucleation events, Tellus B, 53, 344–358, 2001.

Abdul-Razzak, H. and Ghan, S. J.: A parameterization of aerosol activation: 2. Multiple aerosol types, J. Geophys. Res.-Atmos., 105, 6837–6844, 2000.

Ahn, S. H., Yoon, Y. J., Choi, T. J., Lee, J. Y., Kim, Y. P., Lee, B. Y., Ritter, C., Aas, W., Krejci, R., Ström, J., Tunved, P., and Jung, C. H.: Relationship between cloud condensation nuclei (CCN) concentration and aerosol optical depth in the Arctic region, Atmos. Environ., 267, 118748, https://doi.org/10.1016/j.atmosenv.2021.118748, 2021.

Albrecht, B. A.: Aerosols, cloud microphysics, and fractional cloudiness, Science, 245, 1227–1230, 1989.

Anttila, T., Vaattovaara, P., Komppula, M., Hyvärinen, A.-P., Lihavainen, H., Kerminen, V.-M., and Laaksonen, A.: Size-dependent activation of aerosols into cloud droplets at a subarctic background site during the second Pallas Cloud Experiment (2nd PaCE): method development and data evaluation, Atmos. Chem. Phys., 9, 4841–4854, 2009.

Anttila, T., Brus, D., Jaatinen, A., Hyvärinen, A.-P., Kivekäs, N., Romakkaniemi, S., Komppula, M., and Lihavainen, H.: Relationships between particles, cloud condensation nuclei and cloud droplet activation during the third Pallas Cloud Experiment, Atmos. Chem. Phys., 12, 11435–11450, 2012.

Asmi, E., Kivekäs, N., Kerminen, V.-M., Komppula, M., Hyvärinen, A.-P., Hatakka, J., Viisanen, Y., and Lihavainen, H.: Secondary new particle formation in Northern Finland Pallas site between the years 2000 and 2010, Atmos. Chem. Phys., 11, 12959–12972, https://doi.org/10.5194/acp-11-12959-2011, 2011.

Bergman, T., Makkonen, R., Schrödner, R., Swietlicki, E., Phillips, V. T. J., Le Sager, P., and van Noije, T.: Description and evaluation of a secondary organic aerosol and new particle formation scheme within TM5-MP v1.2, Geosci. Model Dev., 15, 683–713, https://doi.org/10.5194/gmd-15-683-2022, 2022.

https://doi.org/10.5194/egusphere-2026-5001
Preprint. Discussion started: 11 September 2026


704 Boucher, O., Randall, D., Artaxo, P., Bretherton, C., Feingold, G., Forster, P., Kerminen, V.-M., Kondo,
705 Y., Liao, H., Lohmann, U., Rasch, P., Satheesh, S. K., Sherwood, S., Stevens, B., and Zhang, X. Y.:
706 Clouds and aerosols, in: Climate Change 2013: The Physical Science Basis. Contribution of Working
707 Group I to the Fifth Assessment Report of the Intergovernmental Panel on Climate Change, edited
708 by: Stocker, T. F., Qin, D., Plattner, G.-K., Tignor, M., Allen, S. K., Boschung, J., Nauels, A., Xia, Y., Bex,
709 V., and Midgley, P. M., Cambridge University Press, Cambridge, UK and New York, NY, USA, 2013.

710 Chang, D., Cheng, Y., Reutter, P., Trentmann, J., Burrows, S. M., Spichtinger, P., Nordmann, S.,
711 Andreae, M. O., Pöschl, U., and Su, H.: Comprehensive mapping and characteristic regimes of aerosol
712 effects on the formation and evolution of pyro-convective clouds, Atmos. Chem. Phys., 15, 10325–
713 10348, https://doi.org/10.5194/acp-15-10325-2015, 2015.

714 Deng, Z. Z., Zhao, C. S., Ma, N., Ran, L., Zhou, G. Q., Lu, D. R., and Zhou, X. J.: An examination of
715 parameterizations for the CCN number concentration based on in situ measurements of aerosol
716 activation properties in the North China Plain, Atmos. Chem. Phys., 13, 6227–6237,
717 https://doi.org/10.5194/acp-13-6227-2013, 2013.

718 Doulgeris, K. M., Vakkari, V., O'Connor, E. J., Kerminen, V.-M., Lihavainen, H., and Brus, D.: Influence
719 of air mass origin on microphysical properties of low-level clouds in a subarctic environment, Atmos.
720 Chem. Phys., 23, 2483–2498, https://doi.org/10.5194/acp-23-2483-2023, 2023.

721 Dusek, U., Frank, G. P., Hildebrandt, L., Curtius, J., Schneider, J., Walter, S., Chand, D., Drewnick, F.,
722 Hings, S., Jung, D., Borrmann, S., and Andreae, M. O.: Size matters more than chemistry for cloud-
723 nucleating ability of aerosol particles, Science, 312, 1375–1378,
724 https://doi.org/10.1126/science.1125261, 2006.

725 Fang, S., Han, Y., Chen, K., Lu, C., Yin, Y., Tan, H., and Wang, J.: Parameterization and comparative
726 evaluation of the CCN number concentration on Mt. Huang, China, Atmos. Res., 181, 300–311,
727 https://doi.org/10.1016/j.atmosres.2016.07.004, 2016.

728 Forster, P., Ramaswamy, V., Artaxo, P., Berntsen, T., Betts, R., Fahey, D. W., Haywood, J., Lean, J.,
729 Lowe, D. C., Myhre, G., Nganga, J., Prinn, R., Raga, G., Schulz, M., and Van Dorland, R.: Changes in
730 atmospheric constituents and in radiative forcing, in: Climate Change 2007: The Physical Science
731 Basis. Contribution of Working Group I to the Fourth Assessment Report of the Intergovernmental
732 Panel on Climate Change, edited by: Solomon, S., Qin, D., Manning, M., Chen, Z., Marquis, M.,
733 Averyt, K. B., Tignor, M., and Miller, H. L., Cambridge University Press, Cambridge, UK and New York,
734 NY, USA, 2007.

735 Gompertz, B.: On the nature of the function expressive of the law of human mortality, and on a new
736 mode of determining the value of life contingencies, Philos. T. R. Soc. Lond., 115, 513–583, 1825.

737 Hari, P., Kulmala, M., Pohja, T., Lahti, T., Siivola, E., Palva, L., Aalto, P., Hämeri, K., Vesala, T., Luoma,
738 S., and Pulliainen, E.: Air pollution in eastern Lapland: challenge for an environmental measurement
739 station, Silva Fenn., 28, 29–39, 1994.

740 Hatakka, J., Aalto, T., Aaltonen, V., Aurela, M., Hakola, H., Komppula, M., Laurila, T., Lihavainen, H.,
741 Paatero, J., Salminen, K., and Viisanen, Y.: Overview of the atmospheric research activities and
742 results at Pallas GAW station, Boreal Environ. Res., 8, 365–383, 2003.

743 Hellén, H., Schallhart, S., Praplan, A. P., Tykkä, T., Aurela, M., Lohila, A., and Hakola, H.:
744 Sesquiterpenes dominate monoterpenes in northern wetland emissions, Atmos. Chem. Phys., 20,
745 7021–7034, https://doi.org/10.5194/acp-20-7021-2020, 2020.

https://doi.org/10.5194/egusphere-2026-5001
Preprint. Discussion started: 11 September 2026


Henning, S., Weingartner, E., Schmidt, S., Wendisch, M., Gäggeler, H., and Baltensperger, U.: Size-dependent aerosol activation at the high-alpine site Jungfraujoch (3580 m a.s.l.), Tellus B, 54, 82–95, 2002.

Hong, J., Häkkinen, S. A. K., Paramonov, M., Äijälä, M., Hakala, J., Nieminen, T., Mikkilä, J., Prisle, N. L., Kulmala, M., Riipinen, I., Bilde, M., Kerminen, V.-M., and Petäjä, T.: Hygroscopicity, CCN and volatility properties of submicron atmospheric aerosol in a boreal forest environment during the summer of 2010, Atmos. Chem. Phys., 14, 4733–4748, 2014.

IPCC: Climate Change 2021: The Physical Science Basis. Contribution of Working Group I to the Sixth Assessment Report of the Intergovernmental Panel on Climate Change, edited by: Masson-Delmotte, V., Zhai, P., Pirani, A., Connors, S. L., Péan, C., Berger, S., Caud, N., Chen, Y., Goldfarb, L., Gomis, M. I., Huang, M., Leitzell, K., Lonnoy, E., Matthews, J. B. R., Maycock, T. K., Waterfield, T., Yelekçi, O., Yu, R., and Zhou, B., Cambridge University Press, Cambridge, United Kingdom and New York, NY, USA, 2391 pp., https://doi.org/10.1017/9781009157896, 2021.

Jaatinen, A., Romakkaniemi, S., Hao, L., Kortelainen, A., Miettinen, P., Mikkonen, S., Smith, J., Virtanen, A., Laaksonen, A., Anttila, T., and Hyvärinen, A.-P.: The third Pallas Cloud Experiment: consistency between the aerosol hygroscopic growth and CCN activity, Boreal Environ. Res., 19, 368–382, 2014.

Karlsson, L., Krejci, R., Koike, M., Ebell, K., and Zieger, P.: A long-term study of cloud residuals from low-level Arctic clouds, Atmos. Chem. Phys., 21, 8933–8959, https://doi.org/10.5194/acp-21-8933-2021, 2021.

Kesselmeier, J. and Staudt, M.: Biogenic volatile organic compounds (VOC): an overview on emission, physiology and ecology, J. Atmos. Chem., 33, 23–88, 1999.

Kivekäs, N., Kerminen, V.-M., Raatikainen, T., Vaattovaara, P., Laaksonen, A., and Lihavainen, H.: Physical and chemical characteristics of aerosol particles and cloud-droplet activation during the Second Pallas Cloud Experiment (Second PaCE), Boreal Environ. Res., 14, 515–526, 2009.

Köhler, H.: The nucleus in and the growth of hygroscopic droplets, Trans. Faraday Soc., 32, 1152–1161, 1936.

Koike, M., Ukita, J., Ström, J., Tunved, P., Shiobara, M., Vitale, V., Lupi, A., Baumgardner, D., Ritter, C., Hermansen, O., Yamada, K., and Pedersen, C. A.: Year-round in situ measurements of Arctic low-level clouds: microphysical properties and their relationships with aerosols, J. Geophys. Res.-Atmos., 124, 1798–1822, https://doi.org/10.1029/2018JD029802, 2019.

Komppula, M., Lihavainen, H., Kerminen, V.-M., Kulmala, M., and Viisanen, Y.: Measurements of cloud droplet activation of aerosol particles at a clean subarctic background site, J. Geophys. Res.-Atmos., 110, D06204, https://doi.org/10.1029/2004JD005200, 2005.

Laj, P., Lund Myhre, C., Riffault, V., Amiridis, V., Fuchs, H., Eleftheriadis, K., Petäjä, T., Salameh, T., Kivekäs, N., Juurola, E., Saponaro, G., Philippin, S., Cornacchia, C., Alados Arboledas, L., Baars, H., Claude, A., De Mazière, M., Dils, B., Dufresne, M., Evangeliou, N., Favez, O., Fiebig, M., Haeffelin, M., Herrmann, H., Höhler, K., Illmann, N., Kreuter, A., Ludewig, E., Marinou, E., Möhler, O., Mona, L., Eder Murberg, L., Nicolae, D., Novelli, A., O'Connor, E., Ohneiser, K., Petracca Altieri, R. M., Picquet-Varrault, B., van Pinxteren, D., Pospichal, B., Putaud, J., Reimann, S., Siomos, N., Stachlewska, I., Tillmann, R., Voudouri, K. A., Wandinger, U., Wiedensohler, A., Apituley, A., Comerón, A., Gysel-Beer, M., Mihalopoulos, N., Nikolova, N., Pietruczuk, A., Sauvage, S., Sciare, J., Skov, H., Svendby, T.,

https://doi.org/10.5194/egusphere-2026-5001
Preprint. Discussion started: 11 September 2026


788 Swietlicki, E., Tonev, D., Vaughan, G., Zdimal, V., Baltensperger, U., Doussin, J., Kulmala, M.,
789 Pappalardo, G., Sorvari Sundet, S., and Vana, M.: Aerosol, Clouds and Trace Gases Research
790 Infrastructure (ACTRIS): the European Research Infrastructure supporting atmospheric science, B.
791 Am. Meteorol. Soc., 105, E1098–E1136, https://doi.org/10.1175/BAMS-D-23-0064.1, 2024.

792 Leck, C., Norman, M., Bigg, E. K., and Hillamo, R.: Chemical composition and sources of the high
793 Arctic aerosol relevant for cloud formation, J. Geophys. Res.-Atmos., 107, AAC 1-1–AAC 1-17,
794 https://doi.org/10.1029/2001JD001463, 2002.

795 Lee, L. A., Pringle, K. J., Reddington, C. L., Mann, G. W., Stier, P., Spracklen, D. V., Pierce, J. R., and
796 Carslaw, K. S.: The magnitude and causes of uncertainty in global model simulations of cloud
797 condensation nuclei, Atmos. Chem. Phys., 13, 8879–8914, https://doi.org/10.5194/acp-13-8879-
798 2013, 2013.

799 Leinonen, V., Kokkola, H., Yli-Juuti, T., Mielonen, T., Kühn, T., Nieminen, T., Heikkinen, S.,
800 Miinalainen, T., Bergman, T., Carslaw, K., Decesari, S., Fiebig, M., Hussein, T., Kivekäs, N., Krejci, R.,
801 Kulmala, M., Leskinen, A., Massling, A., Mihalopoulos, N., Mulcahy, J. P., Noe, S. M., van Noije, T.,
802 O'Connor, F. M., O'Dowd, C., Olivie, D., Pernov, J. B., Petäjä, T., Seland, Ø., Schulz, M., Scott, C. E.,
803 Skov, H., Swietlicki, E., Tuch, T., Wiedensohler, A., Virtanen, A., and Mikkonen, S.: Comparison of
804 particle number size distribution trends in ground measurements and climate models, Atmos. Chem.
805 Phys., 22, 12873–12905, https://doi.org/10.5194/acp-22-12873-2022, 2022.

806 Lohila, A., Penttilä, T., Jortikka, S., Aalto, T., Anttila, P., Asmi, E., Aurela, M., Hatakka, J., Hellén, H.,
807 Henttonen, H., Hänninen, P., Kilkki, J., Kyllönen, K., Laurila, T., Lepistö, A., Lihavainen, H., Makkonen,
808 U., Paatero, J., Rask, M., Sutinen, R., Tuovinen, J.-P., Vuorenmaa, J., and Viisanen, Y.: Preface to the
809 special issue on integrated research of atmosphere, ecosystems and environment at Pallas, Boreal
810 Environ. Res., 20, 431–454, 2015.

811 McCoy, D. T., Bender, F. A.-M., Mohrmann, J. K. C., Hartmann, D. L., Wood, R., and Grosvenor, D. P.:
812 The global aerosol-cloud first indirect effect estimated using MODIS, MERRA, and AeroCom, J.
813 Geophys. Res.-Atmos., 122, 1779–1796, https://doi.org/10.1002/2016JD026141, 2017.

814 Motos, G., Freitas, G., Georgakaki, P., Wieder, J., Li, G., Aas, W., Lunder, C., Krejci, R., Pasquier, J. T.,
815 Henneberger, J., David, R. O., Ritter, C., Mohr, C., Zieger, P., and Nenes, A.: Aerosol and dynamical
816 contributions to cloud droplet formation in Arctic low-level clouds, Atmos. Chem. Phys., 23, 13941–
817 13956, https://doi.org/10.5194/acp-23-13941-2023, 2023.

818 van Noije, T., Bergman, T., Le Sager, P., O'Donnell, D., Makkonen, R., Gonçalves-Ageitos, M.,
819 Döscher, R., Fladrich, U., von Hardenberg, J., Keskinen, J.-P., Korhonen, H., Laakso, A.,
820 Myriokefalitakis, S., Ollinaho, P., Pérez García-Pando, C., Reerink, T., Schrödner, R., Wyser, K., and
821 Yang, S.: EC-Earth3-AerChem: a global climate model with interactive aerosols and atmospheric
822 chemistry participating in CMIP6, Geosci. Model Dev., 14, 5637–5668, https://doi.org/10.5194/gmd-
823 14-5637-2021, 2021.

824 Ovadnevaite, J., Ceburnis, D., Leinert, S., Dall'Osto, M., Canagaratna, M., O'Doherty, S., Berresheim,
825 H., and O'Dowd, C.: Submicron NE Atlantic marine aerosol chemical composition and abundance:
826 seasonal trends and air mass categorization, J. Geophys. Res.-Atmos., 119, 11850–11863, 2014.

827 Petters, M. D. and Kreidenweis, S. M.: A single parameter representation of hygroscopic growth and
828 cloud condensation nucleus activity, Atmos. Chem. Phys., 7, 1961–1971, 2007.

https://doi.org/10.5194/egusphere-2026-5001
Preprint. Discussion started: 11 September 2026


Petäjä, T., Tabakova, K., Manninen, A., Ezhova, E., O'Connor, E., Moisseev, D., Sinclair, V. A., Backman, J., Levula, J., Luoma, K., Virkkula, A., Paramonov, M., Räty, M., Äijälä, M., Heikkinen, L., Ehn, M., Sipilä, M., Yli-Juuti, T., Virtanen, A., Ritsche, M., Hickmon, N., Pulik, G., Rosenfeld, D., Worsnop, D. R., Bäck, J., Kulmala, M., and Kerminen, V.-M.: Influence of biogenic emissions from boreal forests on aerosol–cloud interactions, Nat. Geosci., 15, 42–47, 2022.

Pierce, J. R. and Adams, P. J.: Uncertainty in global CCN concentrations from uncertain aerosol nucleation and primary emission rates, Atmos. Chem. Phys., 9, 1339–1356, https://doi.org/10.5194/acp-9-1339-2009, 2009.

Platt, S. M., Hov, Ø., Berg, T., Breivik, K., Eckhardt, S., Eleftheriadis, K., Evangeliou, N., Fiebig, M., Fisher, R., Hansen, G., Hansson, H.-C., Heintzenberg, J., Hermansen, O., Heslin-Rees, D., Holmén, K., Hudson, S., Kallenborn, R., Krejci, R., Krognes, T., Larssen, S., Lowry, D., Lund Myhre, C., Lunder, C., Nisbet, E., Nizzetto, P. B., Park, K.-T., Pedersen, C. A., Aspmo Pfaffhuber, K., Röckmann, T., Schmidbauer, N., Solberg, S., Stohl, A., Ström, J., Svendby, T., Tunved, P., Tørnkvist, K., van der Veen, C., Vratolis, S., Yoon, Y. J., Yttri, K. E., Zieger, P., Aas, W., and Tørseth, K.: Atmospheric composition in the European Arctic and 30 years of the Zeppelin Observatory, Ny-Ålesund, Atmos. Chem. Phys., 22, 3321–3369, https://doi.org/10.5194/acp-22-3321-2022, 2022.

Prank, M., Sofiev, M., Denier van der Gon, H. A. C., Kaasik, M., Ruuskanen, T. M., and Kukkonen, J.: A refinement of the emission data for Kola Peninsula based on inverse dispersion modelling, Atmos. Chem. Phys., 10, 10849–10865, https://doi.org/10.5194/acp-10-10849-2010, 2010.

Rantanen, M., Karpechko, A. Y., Lipponen, A., Nordling, K., Hyvärinen, O., Ruosteenoja, K., Vihma, T., and Laaksonen, A.: The Arctic has warmed nearly four times faster than the globe since 1979, Commun. Earth Environ., 3, 168, https://doi.org/10.1038/s43247-022-00498-3, 2022.

Reutter, P., Su, H., Trentmann, J., Simmel, M., Rose, D., Gunthe, S. S., Wernli, H., Andreae, M. O., and Pöschl, U.: Aerosol- and updraft-limited regimes of cloud droplet formation: influence of particle number, size and hygroscopicity on the activation of cloud condensation nuclei (CCN), Atmos. Chem. Phys., 9, 7067–7080, https://doi.org/10.5194/acp-9-7067-2009, 2009.

Roberts, G. C. and Nenes, A.: A continuous-flow streamwise thermal-gradient CCN chamber for atmospheric measurements, Aerosol Sci. Technol., 39, 206–221, https://doi.org/10.1080/027868290913988, 2005.

Sanchez, K. J., Chen, C.-L., Russell, L. M., Betha, R., Liu, J., Price, D. J., Massoli, P., Ziemba, L. D., Crosbie, E. C., Moore, R. H., Müller, M., Schiller, S. A., Wisthaler, A., Lee, A. K. Y., Quinn, P. K., Bates, T. S., Porter, J., Bell, T. G., Saltzman, E. S., Vaillancourt, R. D., and Behrenfeld, M. J.: Substantial seasonal contribution of observed biogenic sulfate particles to cloud condensation nuclei, Sci. Rep., 8, 3235, 2018.

Schmale, J., Henning, S., Henzing, B., Keskinen, H., Sellegri, K., Ovadnevaite, J., Bougiatioti, A., Kalivitis, N., Stavroulas, I., Jefferson, A., Park, M., Schlag, P., Kristensson, A., Iwamoto, Y., Pringle, K., Reddington, C., Aalto, P., Äijälä, M., Baltensperger, U., Bialek, J., Birmili, W., Bukowiecki, N., Ehn, M., Fjæraa, A. M., Fiebig, M., Frank, G., Fröhlich, R., Frumau, A., Furuya, M., Hammer, E., Heikkinen, L., Herrmann, E., Holzinger, R., Hyono, H., Kanakidou, M., Kiendler-Scharr, A., Kinouchi, K., Kos, G., Kulmala, M., Mihalopoulos, N., Motos, G., Nenes, A., O'Dowd, C., Paramonov, M., Petäjä, T., Picard, D., Poulain, L., Prévôt, A. S. H., Slowik, J., Sonntag, A., Swietlicki, E., Svenningsson, B., Tsurumaru, H., Wiedensohler, A., Wittbom, C., Ogren, J. A., Matsuki, A., Yum, S. S., Lund Myhre, C., Carslaw, K., Stratmann, F., and Gysel, M.: Collocated observations of cloud condensation nuclei, particle size

https://doi.org/10.5194/egusphere-2026-5001
Preprint. Discussion started: 11 September 2026


distributions, and chemical composition, Sci. Data, 4, 170003, https://doi.org/10.1038/sdata.2017.3, 2017.

Schulzweida, U.: CDO User Guide, Zenodo, https://doi.org/10.5281/zenodo.10020800, 2023.

Sipilä, M., Sarnela, N., Neitola, K., Laitinen, T., Kemppainen, D., Beck, L., Duplissy, E.-M., Kuittinen, S., Lehmusjärvi, T., Lampilahti, J., Kerminen, V.-M., Lehtipalo, K., Aalto, P. P., Keronen, P., Siivola, E., Rantala, P. A., Worsnop, D. R., Kulmala, M., Jokinen, T., and Petäjä, T.: Wintertime subarctic new particle formation from Kola Peninsula sulfur emissions, Atmos. Chem. Phys., 21, 17559–17576, https://doi.org/10.5194/acp-21-17559-2021, 2021.

Stein, A. F., Draxler, R. R., Rolph, G. D., Stunder, B. J. B., Cohen, M. D., and Ngan, F.: NOAA's HYSPLIT atmospheric transport and dispersion modeling system, B. Am. Meteorol. Soc., 96, 2059–2077, 2015.

Stier, P., Feichter, J., Kinne, S., Kloster, S., Vignati, E., Wilson, J., Ganzeveld, L., Tegen, I., Werner, M., Balkanski, Y., Schulz, M., Boucher, O., Minikin, A., and Petzold, A.: The aerosol-climate model ECHAM5-HAM, Atmos. Chem. Phys., 5, 1125–1156, https://doi.org/10.5194/acp-5-1125-2005, 2005.

Twomey, S.: Influence of pollution on the shortwave albedo of clouds, J. Atmos. Sci., 34, 1149–1152, 1977.

Vignati, E., Wilson, J., and Stier, P.: M7: an efficient size-resolved aerosol microphysics module for large-scale aerosol transport models, J. Geophys. Res.-Atmos., 109, D22202, https://doi.org/10.1029/2003JD004485, 2004.

Virkkula, A., Hillamo, R. E., Kerminen, V.-M., and Stohl, A.: The influence of Kola Peninsula, continental European and marine sources on the number concentrations and scattering coefficients of the atmospheric aerosol in Finnish Lapland, Boreal Environ. Res., 2, 317–336, 1997.

Virtanen, A., Joutsensaari, J., Kokkola, H., Partridge, D. G., Blichner, S., Seland, Ø., Holopainen, E., Tovazzi, E., Lipponen, A., Mikkonen, S., Leskinen, A., Hyvärinen, A.-P., Zieger, P., Krejci, R., Ekman, A. M. L., Riipinen, I., Quaas, J., and Romakkaniemi, S.: High sensitivity of cloud formation to aerosol changes, Nat. Geosci., 18, 289–295, https://doi.org/10.1038/s41561-025-01662-y, 2025.

Väisänen, O., Ruuskanen, A., Ylisirniö, A., Miettinen, P., Portin, H., Hao, L., Leskinen, A., Komppula, M., Romakkaniemi, S., Lehtinen, K. E. J., and Virtanen, A.: In-cloud measurements highlight the role of aerosol hygroscopicity in cloud droplet formation, Atmos. Chem. Phys., 16, 10385–10398, https://doi.org/10.5194/acp-16-10385-2016, 2016.

Wang, Y., Neubauer, D., Chen, Y., Jordan, G., Malavelle, F., Yuan, T., Partridge, D., Field, P., Wang, H., Wang, M., Michou, M., Nabat, P., Laakso, A., Myhre, G., and Lohmann, U.: Challenges in global climate models to represent cloud response to aerosols: insights from volcanic eruptions, Nat. Commun., 17, 627, https://doi.org/10.1038/s41467-025-67359-3, 2026.

Yang, F., McGraw, R., Luke, E. P., Zhang, D., Kollias, P., and Vogelmann, A. M.: A new approach to estimate supersaturation fluctuations in stratocumulus cloud using ground-based remote-sensing measurements, Atmos. Meas. Tech., 12, 5817–5828, https://doi.org/10.5194/amt-12-5817-2019, 2019.

Yli-Juuti, T., Mielonen, T., Heikkinen, L., Arola, A., Ehn, M., Isokääntä, S., Keskinen, H.-M., Kulmala, M., Laakso, A., Lipponen, A., Luoma, K., Mikkonen, S., Nieminen, T., Paasonen, P., Petäjä, T., Romakkaniemi, S., Tonttila, J., Kokkola, H., and Virtanen, A.: Significance of the organic aerosol driven climate feedback in the boreal area, Nat. Commun., 12, 5637, 2021.